Universidade do Minho
Escola de Engenharia

Bruno Pacheco Fernandes

Preparation of particles for cosmetic applications in human hair

Outubro de 2012

Preparation of particles for cosmetic applications in human hair
Bruno Pacheco Fernandes
UMinho | 2012

Universidade do Minho
Escola de Engenharia

Bruno Pacheco Fernandes

Preparation of particles for cosmetic applications in human hair

Tese de Mestrado
Micro/Nano Tecnologias

Trabalho efectuado sob a orientação do
Professor Doutor Artur Manuel Cavaco-Paulo

e coorientação da
Doutora Raquel de Jesus Marques da Silva

Outubro de 2012

“The scientist is not a person who gives the right answers, he is one who asks the right questions.”

Claude Lévi-Strauss

To my Parents

ACKNOWLEDGMENTS

Now that this stage of my education is coming to an end, it is time to express my gratitude to all those who, in this last year, contributed for the success of this journey.

I thank to Professor Artur Cavaco-Paulo for the opportunity to work on his research group, for trusting in me to accomplish this project, for his support and guidance as well as for his availability. I am also grateful to Dra. Raquel Silva, my co-supervisor, for the dedication and manifested patience, for the knowledge transmitted and for all the constructive comments and suggestions that helped me in the challenges of this work and improved the writing of my thesis.

To my colleagues in the Bioprocess Research Group, I express my appreciation for the help, for never refusing to take my doubts and for the excellent work environment they provided to me. A special thanks to Artur Ribeiro for the valuable assistance in the last part of this work.

For the support, for always being there for me and for emotionally raise me up, thank you to all my friends, especially to those who are closest to me: Ademar, Carina, Félix, Laura and Nuno. For helping me with the fluorescence microscope, I also thank to Rita.

I also want to show gratitude to my amazing family because of the endless support I received from them since ever. To my cousin Carla, a special thanks for the laptop you lent me when mine broke down, allowing me to write the thesis on time.

And last but not least, my most heartfelt recognition goes to my parents for their unconditional love and care, for teaching me to be who I am, for always support my choices and without whom this thesis would not exist.

Thank you all!

Preparation of particles for cosmetic applications in human hair

ABSTRACT

Nanoparticles (NPs) have a huge interest for transdermal applications, demonstrating their ability to be trapped in the hair follicles (HFs) where they release the entrapped compounds. For hair cosmetics, this discovery is particularly important as it can improve the treatment of several hair follicle related disorders/diseases. Therefore, the aim of this work was to obtain NPs of Poly (Lactic Acid) (PLA-NPs) for topical delivery of drugs at the level of the HFs. Further, these particles may be used for cosmetic applications in human hair.

The effect of several parameters was examined, in order to establish an improved nanoprecipitation protocol for the preparation of suitable PLA carriers for follicular targeting. Thus, the application of mechanical stirring or ultrasound, the use of Acetone/Ethanol (50/50, v/v) as the solvent phase and the addition of 0.6% (w/w) of Pluronic F68 to the formulation showed the best compromise between the desired properties (monodispersed populations of particles with a mean size of ≈150 nm were obtained, the ζ-potential was less than -18 mV and particles exhibited a spherical shape with smooth surface) and the yield of nanoparticles (≈90% was showed for particles produced with agitation and ≈70% when ultrasound was employed).

After the encapsulation of model compounds, no significant changes were found in the properties of particles and the entrapment efficiency was above 80%. Nevertheless, the use of sonication promoted higher loading efficiencies. In turn, the release kinetics of PLA nanoparticles indicated an anomalous dye transport mechanism (diffusion and polymer degradation) for Nile Red (lipophilic) and a Fickian diffusion of first order for FITC (hydrophilic). Furthermore, the release from particles produced with agitation was slightly faster than from particles produced with sonication.

Finally, fluorescence microscopy on porcine skin cryosections showed that the produced PLA-NPs can effectively transport lipophilic and hydrophilic compounds into the HFs, with fluorochromes reaching a maximal depth corresponding to the full follicles length after 24h.

In conclusion, the modified nanoprecipitation protocol presented in this study allows the preparation of PLA nanocarriers with potential for hair follicle therapy and the yields obtained are acceptable for industrial purposes.

Preparação de partículas para aplicações cosméticas em cabelo humano

RESUMO

As nanopartículas (NPs) são de grande interesse para aplicações transdérmicas, acumulando-se nos folículos capilares (FC) onde libertam os compostos encapsulados. Esta descoberta é particularmente importante para a cosmética capilar, podendo melhorar o tratamento de várias doenças/distúrbios associados aos FC. Consequentemente, este trabalho visou a obtenção de NPs de Poli (Ácido Lático) (PAL-NPs) para entrega de agentes terapêuticos ao nível dos FC. No futuro, estas partículas poderão ser utilizadas para aplicações cosméticas em cabelo humano.

Inicialmente, o efeito de algumas variáveis experimentais foi testado, de modo a melhorar o protocolo de nanoprecipitação para a produção de PAL-NPs aptas para entrega de princípios ativos ao nível dos FC. Assim, a melhor relação entre as propriedades desejadas e o rendimento em nanopartículas foi obtida com a aplicação de agitação mecânica ou ultrassons, o uso de Acetona/Etanol (50/50, v/v) como fase solvente e a adição de 0.6% (w/w) de Pluronic F68 à formulação. Com estas condições obtiveram-se populações monodispersas de partículas esféricas com uma superfície lisa, tamanhos médios de 150 nm, carga superficial inferior a -18 mV e rendimentos de ≈90% e ≈70% para partículas produzidas com agitação e sonicação, respetivamente.

Após um encapsulamento eficiente (> 80%) do Nile Red e do FITC, não foram registadas alterações significativas nas propriedades das partículas. Por sua vez, o mecanismo de libertação dos compostos mostrou-se dependente da sua natureza: para o Nile Red (lipofílico) ocorreu transporte anómalo (difusão e degradação do polímero) e a libertação do FITC (hidrofílico) foi controlada por difusão fickiana de primeira ordem. É também de salientar que a libertação dos fluorocromos foi ligeiramente mais rápida para partículas produzidas com agitação.

Por último, usando microscopia de fluorescência em secções de pele de porco, provou-se que as NPs produzidas são eficazes no transporte de compostos lipofílicos e hidrofílicos para o interior dos FC. Mais ainda, ao fim de 24h foi possível detetar a presença dos corantes ao longo de toda a extensão destas estruturas.

Em suma, as alterações introduzidas ao protocolo de nanoprecipitação permitiram a preparação de nanopartículas de PAL com potencial para terapia folicular sendo que, os rendimentos obtidos são aceitáveis para aplicação industrial.

TABLE OF CONTENTS

LIST OF ABBREVIATIONS

A

ACS	American Chemical Society
approx.	Approximately

C

°C	Celsius

D

Da	Dalton
DDS	Drug Delivery Systems
DGV	Direção Geral de Veterinária
DMSO	Dimethyl sulfoxide

E

e.g.	For example

F

FDA	Food and Drug Administration
FITC	Fluorescein 5(6)-isothiocyanate

G

g	Gram

H

HF	Hair Follicle(s)
h	Hours
HPLC	High Performance Liquid Chromatography

I

IPM	Isopropyl Myristate

K

kV	Kilovolts
kHz	Kilohertz

L

LDA	Laser Doppler Anemometry

M

µL	Microliters
µm	Micrometers
m	Meters
MEC	Minimum Effective Concentration
min	Minutes
mL	Milliliters
mm	Millimeters
MTC	Minimum Toxic Concentration
mV	Millivolts

N

nm	Nanometers
NP(s)	Nanoparticle(s)
NR	Nile Red

O

o/w	Oil in water
$^{\bullet}$OH	Hydroxyl radical

P

PBS	Phosphate Buffered Saline Solution
PCL	Poly-ε-caprolactone
PCS	Photon Correlation Spectroscopy
PDI	Polydispersity Index

PLA	Poly (Lactic Acid)/Poly (D, L-Lactic Acid)
PLA-NPs	Nanoparticles of Poly (D, L-Lactic Acid)
PLGA	Poly Lactic-co-glycolic Acid
Pluronic F68	Pluronic acid F68

R

rpm	Rotations per minute

S

SC	*Stratum Corneum*
SESD	Spontaneous Emulsion Solvent Diffusion
SLN	Solid Lipid Nanoparticles
s	Second
STEM	Scanning Transmission Electron Microscopy
SD	Standard Deviation

U

UV	Ultraviolet
UV-Vis	Ultraviolet-Visible

V

v/v	Volume/volume

W

w/o	Water in oil
w/o/w	Water in oil in water
w/v	Weight/volume
w/w	Weight/weight

Z

ζ-potential	Zeta-Potential

LIST OF FIGURES

LIST OF TABLES

LIST OF EQUATIONS

1. MOTIVATION AND AIMS OF THE STUDY

Nanotechnology is an interdisciplinary area that deals with the development, manipulation and control of materials at nanometric scale, in order to take advantage of their singular physical, chemical and biological properties [1, 2]. Currently, due to the many new options that this scale can offer, nanotechnology is a key field of research, providing means for achieving otherwise unreachable goals [3, 4].

The cosmetic industry was among the first to use nanotechnology in the development of products. From 1994 to 2005, L'Oreal SA (France) was worldwide ranked in 5th placed on the total number of nanotechnology-based products and in 2009, more than 13% of nanostructured products available in the market were classified for cosmetic use [4]. This growing interest in the development of nanotechnological cosmetics occurred because nanomaterials have the potential to radically change the way cosmetics deliver their benefits, leading to product innovation, which consequently may stimulate the economy of one of the most important worldwide industries [5, 6].

Among nanomaterials for cosmetic use, nanoparticles (NPs) are of particular interest because they improve the stability of various cosmetic ingredients like unsaturated fatty acids, enhance the penetration of certain agents as vitamin and other oxidants, increase the efficacy and tolerance of UV filters on the skin surface and make the product more aesthetically pleasing [7]. Moreover, NPs are also important for cosmetic applications because they can encapsulate a wide range of ingredients as vitamins, fragrances, and drugs with cosmetic or dermatological purposes and act as Drug Delivery Systems (DDS) [5].

Regarding to the route of administration, for cosmetic applications but not only, the transport of DDS through the skin has been widely studied because it offers numerous advantages over other routes [8]. After topical application, although nanoparticles may accumulate at different skin sites depending on their properties, they tend to be trapped inside the hair follicles (HFs), reaching high concentrations at these sites [9]. This localized accumulation of nanoparticles is very important for hair cosmetics because, using NPs it will be possible to achieve adequate concentrations of active ingredients into these structures, in order to treat many hair follicle related disorders/diseases without damages to the hair or skin lesions [10].

The present study aimed to obtain nanoparticles that could be used as carriers for topical delivery of drugs at the level of the HFs. Thus, these particles may be used for cosmetic applications in human hair. Initially, to achieve the ultimate goal proposed, the influence of several experimental factors was tested in order to obtain an adequate formulation for the production of Poly (D,L-Lactic Acid) nanoparticles (PLA-NPs) by nanoprecipitation methodology. The yield of nanoparticles was further determined and the entrapment efficiency and release profile of hydrophilic and lipophilic compounds from PLA-NPs were achieved. Finally, the ability of these particles to penetrate the skin and accumulate in the HFs was assessed *in vitro*.

2. REVIEW OF THE LITERATURE

2.1. Nanoparticles as Carriers for Drug Delivery

In the last decades, significant advances have been made in the production of nanoparticles (NPs) as carriers to deliver therapeutic agents into the body [11]. Thus, the application of nanotechnology on drug delivery enabled the creation of entirely new therapeutic agents [12].

The main advantage of NPs as drug delivery systems (DDS) is their ability to target specific cell populations in the human body and to help in the intracellular uptake of the drugs [13]. The efficiency of drug delivery to various parts of the body is directly affected by particle size but it can be modulated through the modification of particle surface (e.g., binding to specific ligands as monoclonal antibodies to target a selected cell population) [11]. By providing a high local concentration just at the desired site of action, NPs enhance the bioavailability of drugs, minimizing the amount of active substances needed. The application of a low dose of drugs reduces the risk of side-effects in other tissues and it makes possible to use certain drugs that were previously impractical because of their toxicities [11, 13, 14]. Another important feature of NPs is their capacity to promote a sustained drug release over a prolonged period of time [11]. Controlling the drug carrier architecture (e.g., porosity), the release of the drug can be tuned to achieve a desired kinetic profile, fixating the concentration of the encapsulated substance between the Minimum Effective Concentration (MEC) and the Minimum Toxic Concentration (MTC), for an adequate period of time (Figure 2-1); achieving a constant drug level in tissues, the therapeutic index (ratio between the efficacy of the drug and its undesirable side effects) is maximized [11, 13, 15]. In conventional systems, many applications are need to maintain the drug level above MEC (otherwise there is no beneficial effect) and bellow MTC (above this limit, the active substance becomes toxic) because, following a relatively short period at the therapeutic level, drug concentration drops off until re-administration [15, 16]. Thus, NPs can reduce the frequency of drug administration, increasing the consumer's compliance and acceptance [11]. Finally, nanoparticles can also provide protection to the encapsulated drugs, making them more stables, resulting in the maintenance of their bioactivity until they reach the target [17, 18].

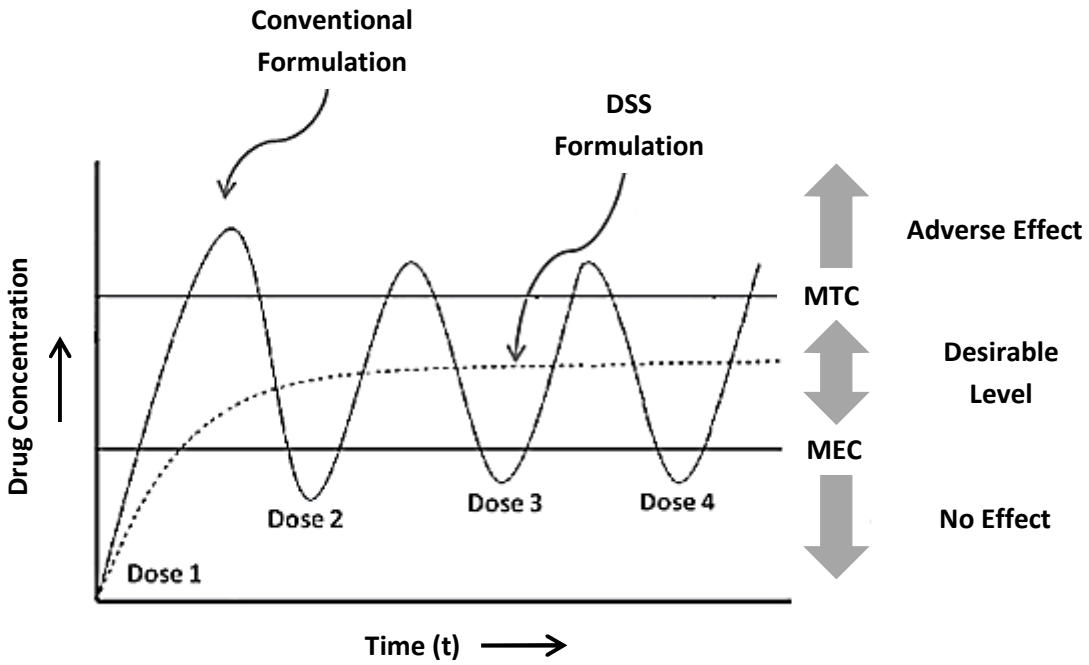

Figure 2-1: Release profile of conventional formulation and drug delivery systems (DDS), over time (Adapted from Das S. *et al.*, 2011 [19]).

A broad range of materials like lipids, proteins, metals and polymers have been studied for the production of nanoparticles [11]. The choice of the material must to take into account their biodegradability and biocompatibility because *in vivo* degradation must be fast, originating products that can be metabolized and eliminated by the organism [15]. A careful choice of material is also important once that it will affect the properties of target and controlled release of nanoparticles [18]. To synthetize the particles, numerous protocols are already described based on the type of material, type of drug used or the desired delivery route and several structures like liposomes, micelles, solid lipid nanoparticles (SLN), dendrimers and polymeric nanoparticles were already obtained and reported as efficient systems for delivery purposes [11, 20]. Liposomes are hollow particles, composed of one or several closed phospholipid bilayers offering a hydrophobic shell (lipid layer) as well as a hydrophilic core (inner volume of the liposome); lipophilic and hydrophilic substances can be integrated into the shell or the core, respectively [3, 5, 11, 21]. Micelles are structures smaller than liposomes, which has either a fatty core separated from an aqueous

solvent by the polar heads (normal micelle) or else an aqueous core separated by the polar heads from a fatty solvent (inverse micelle) [3]. SLNs are formed by a matrix of lipids which are biodegradable raw materials that are physiological well tolerated [22]. Dendrimers, a unique class of polymers, are highly branched macromolecules whose size and shape can be precisely controlled [13]. Finally, polymeric nanoparticles have a core surrounded by a polymeric shell and generally, they exhibit greater stability [23]. While there is plenty of research in the production of nanoparticles for drug delivery, only a few of them have reached the market because they are still several limitations associated with the design and characterization of these materials (ability to reproducibly fabricate specific nanoparticle shapes and sizes, to achieve optimal drug loading of carrier, to control drug release and delivery and to design stable materials, which do not release harmful degradation products) [14, 24]. The initial cost of materials and the expensive processes also has limited the commercial distribution of these systems [15]. However, the remarkable results achieved with nanoparticulate DSS in animal models are promising for their extensive commercialization in the coming years [11].

The administration of nanoparticulate DSS to humans can be made through injection or across oral, pulmonary, ocular, transmucosal and dermal routes [13]. Lately, special attention has been given to the transport of drugs through the skin (topical application), because this route offers a lot of vantages when compared, for example, to intravenous injection or oral administration [8]. The administration of nanoparticles through the skin is particularly important in the field of cosmetic, once those particles had proved to be valuable for optimizing current galenical formulations for topical dermatotherapy [11].

2.2. Drug Administration through the Skin

The main function of the skin is to provide a protective barrier against external agents; however, its passive diffusion mechanism can also allow the penetration of substances, making it a potential route for the delivery of drugs into the

body [25, 26]. According to the purpose, the delivery through the skin can be divided into topical and transdermal delivery; topical delivery involves drug administration for local therapeutic effects, whereas transdermal delivery uses the skin as a route for the transport of drugs into the circulatory system [27].

The skin offers many advantages over other routes of drug administration because it is a large and readily accessible surface area for absorption, the application is a noninvasive procedure (allowing continuous intervention) and it is possible to cease the absorption preventing overdose or undesirable effects [28]. When compared with the traditional oral route of drug administration, additional advantages are shown: it avoids the gastrointestinal tract (and consequently, drug degradation under the extreme acidity of the stomach), it avoids hepatic first pass metabolism (increasing the bioavailability of drug) and it reduces the fluctuations on the drugs level in the plasma, minimizing the risk of systemic side effects [25, 28]. Despite all the advantages of drug administration through the skin, this route also has some disadvantages such as, higher molecular weight candidates fail to penetrate without modifying the nature of skin, drugs with very low or high partition coefficient fail to reach systemic circulation and high melting drugs have difficult to permeate due to their low solubility in the skin [25]. Therefore, to make these compounds suitable for topical administration is necessary to increase skin permeability or increase solubility of drugs in the skin [28].

2.2.1. Approaches to Overcoming the Dermal Barrier

Chemical and physical methods have been aimed to disrupt or weaken the skin in an attempt to enhance drug transport across it [29]. Physical enhancement methods usually involve the use of an energy source to overcome the barrier properties of the skin and include iontophoresis (driving charged molecules into the skin by a small direct current), electroporation (application of short micro- to milli-second electrical pulses to create transient pores in skin) and sonophoresis (cavitation caused by low frequency ultrasound energy, which increases skin fluidity) [28, 30, 31].

Alternative physical approaches to increase skin permeability, without the use of an energy source, involves the use of microneedles (which can be inserted into the skin producing a channel for drug transport), jet-propelled particles (high-velocity jet of compressed gas carrying drug particles) and ablation of the *stratum corneum* [30, 31]. For chemical enhancing of percutaneous absorption, water is the safest and most widely used penetration enhancer; the increasing of hydration leads to a diminished resistance of the skin [25]. Other chemical enhancers, which promote changes in the structure of skin, have also been reported [32]. These chemicals can disrupt the lipid organization of skin (e.g., azone, terpenes, fatty acids, dimethyl sulfoxide (DMSO) and alcohols) or alter its protein organization (DMSO or urea) [28]. Although these methods have proved to be effective for increase skin permeability to drugs, they also induce irritation and they cause damages to the skin, reducing its barrier function [32].

2.2.2. Nanotechnology for Conquering the Skin Barrier

Since an ideal penetration enhancer should reversibly reduce the barrier resistance of skin without damaging it, nanoparticulate DSS are the most promising alternative to the physical and chemical penetration enhancer systems [14, 32, 33]. Nanoparticles can modify the physicochemical properties of the encapsulated molecules and offer a means to facilitate the percutaneous delivery of substances, increasing the permeability and transport of therapeutic agents into/across the skin without damaging it [14, 26, 32, 33]. NPs can also protect drugs from be metabolized by mircoflora or enzymes on the surface of skin and prevent allergic responses in skin induced by the encapsulated drugs [25].

Despite the advances in recent years, the transport of a wide range of drugs through the skin is still limited due to the special composition and structure of skin, which provides a formidable barrier to penetration [25, 31, 34]. Thus, explore and understanding the anatomy, physiology and chemical composition of the skin is important to improve the nanoparticles design and increase the ability to deliver these materials with wide systemic and topical application [14, 28]. An understanding of the

interactions between these novel drug delivery systems and the skin, as well as the transport pathways within the skin, is also required to establish the feasibility of using nanoparticles to optimize the transport process [33].

2.3. The Dermal Barrier

The skin, or *cutis*, is considered the largest human organ; being normally less than 2 mm thin, it accounts more than 10% of the body mass and have an average surface of approximately 2 m^2. This organ enables the body to interact dynamically with the environment and plays many functions (protective, homeostatic and sensorial), essential for the survival of the human beings [35]. Specifically, the excellent protective/biological barrier function of skin protects the body against external mechanical, chemical, microbial and physical influences [3]. To maintain its characteristics, this organ is in a continual renewing process [28].

Because of large surface area and easy accessibility, skin delivery has potential application in drug delivery [36]. However, the functional properties that enable skin to act as an excellent barrier also serve to limit the access of drugs into and across it [28]. Whereas an initial consideration of the skin structure might suggest a simple barrier, a closer examination reveals a complex combination of a range of cell types [31]. Thus, to optimize the delivery of drugs into or across the skin is important to learn its structure, in order to learn how to overcoming its barrier function [37].

2.3.1. The Structure of the Skin

The Figure 2-2 shows the structure of the skin. Anatomically, it is composed of epidermis, dermis and hypodermis (also called subcutaneous tissue), being a complex barrier as a consequence of its anatomical organization and special chemical composition [22, 27]. In addition to these main layers, several pilosebaceous units (hair follicles and associated sebaceous glands) and apocrine or eccrine sweat glands are

dispersed throughout the skin [14, 36]. Owing to its unique biochemical and anatomical properties, each individual skin layer is mechanically different [3].

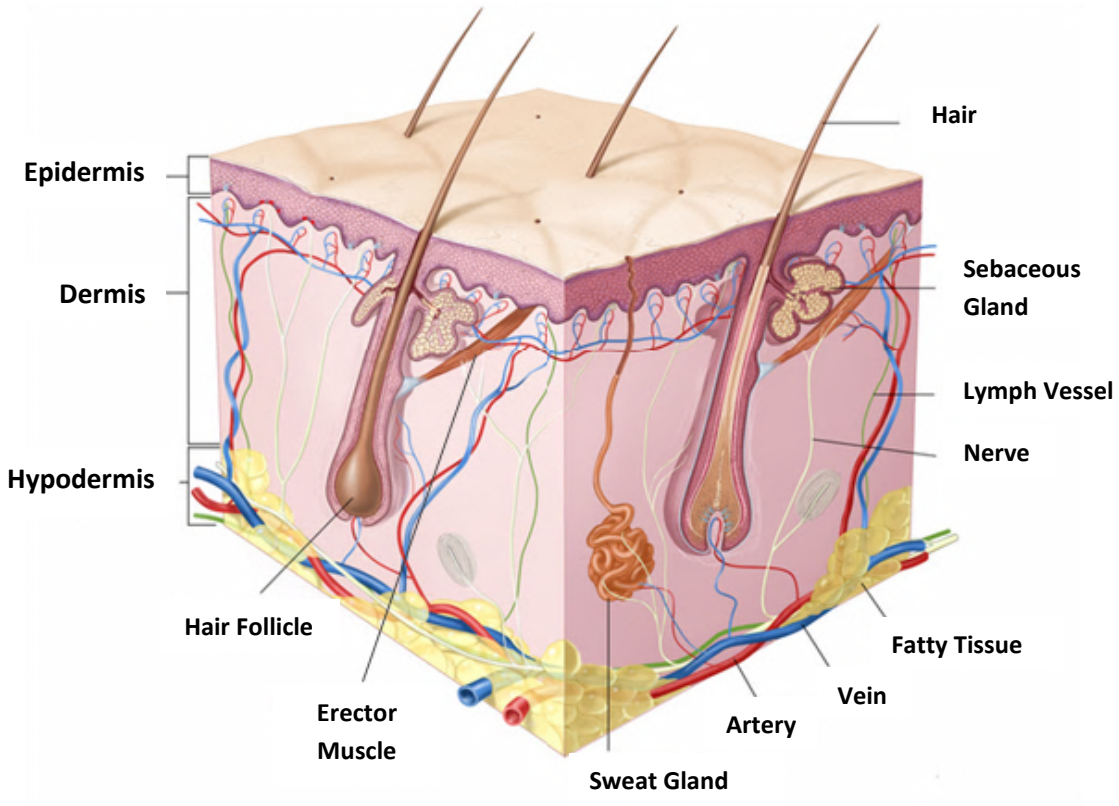

Figure 2-2: Anatomy of the skin (Online image, available at http://www.meb.uni-bonn.de/Cancernet/Media/CDR0000579036.jpg; accessed on September 10, 2012).

The innermost layer, the hypodermis, is composed of loose textured, white, fibrous connective tissue in which fat and elastic fibers are intermingled [36]. This layer acts as insulator, shock absorber, and reserve depot of calories and supplier of nutrients for the more superficial skin layers [37]. On its domain, it can be found the base of the hair follicles, the secretory portion of the sweat glands, the cutaneous nerves and the networks of lymph and blood vessels [28].

Above the hypodermis, there is dermis which normally measure up to 2 mm in thickness [3]. The dermis is a fibrous layer that supports and strengthens the epidermis and it consists of a matrix of loose connective tissue composed by collagen (a fibrous

protein) embedded in a semigel matrix, which contains water, ions and mucopolysaccharides; this matrix allows the oxygen and nutrients to diffuse to the epidermal cells [37]. The dermis shelters a network of blood capillaries, lymphatic vessels, nerve endings and nearly all elastic fibers giving mechanical stability to the skin [36]. Finally, this region of skin contains only few cells, predominantly fibroblasts (responsible for the connective tissue synthesis), mast cells (involved in the immune and inflammatory responses) and melanocytes (involved in the production of melanin) [37].

The top layer of the skin (epidermis) is typically 50-150 μm thin and it contains four histologically distinct strata of keratinocytes, which varying in the differentiation level [3, 37]. The innermost *Stratum Basale* is composed of two keratinocyte types, one that acts as stem cells having a proliferation capacity, and the second one which serves as anchor to the basement membrane; in this strata is also possible to find Merkel cells (sensory perception), Langerhans cells (immunological function) and melanocytes (melanin production) [14, 36]. During the differentiation process to form the higher epidermal layers, keratinocytes undergo a process of keratinization, in which the cell differentiates and moves upward from *Stratum Basale*, through the *Stratum Spinosum* and *Stratum Granulosum*, to the outermost layer, the *Stratum Corneum* (SC), also called horny layer or non-viable epidermis [14]. Therefore, the SC represents the final stage of epidermal cell differentiation and it has an approximately thickness of 5 - 20 μm but a number of factors, including the degree of hydration and skin location, can influence it [29, 37]. This layer is the main responsible for the resilient absorption properties of skin, providing protection to the body against the entry of external materials but it is also the main barrier for diffusion of water out of the skin [14, 27, 36].

2.3.1.1. Organization of the *Stratum Corneum*

The structure of SC has been described by “brick and mortar” model (Figure 2-3) and it was first presented by Michaels *et al.* [38].

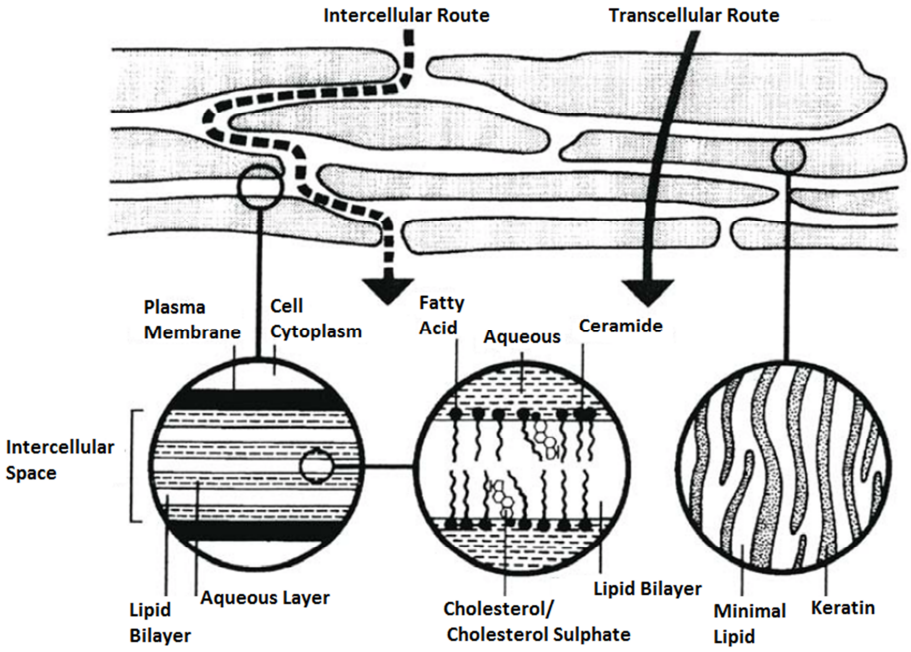

Figure 2-3: Schematic representation of the "brick and mortar" model of the *stratum corneum* (Adapted from Moghimi H.R. *et al,* 1996 [39]).

The "bricks" of the model correspond to hydrophilic corneocytes (also called horny cells) which are dead, anuclear, flattened and hexagonal cells [14, 27, 28]. They are composed mainly of insoluble bundled keratins (70%) and lipids (approx. 20%); their approximate diameter and thickness is 40 µm and 0.5 µm, respectively [28, 37]. In SC, corneocytes are vertically stacked into columns (perpendicular to the skin surface) and each column contains between 10 and 15 cellular layers of keratinized cells. The "bricks" are joined together by desmosomes, which help to form a tough outer layer by maintaining cellular shape and regular packing [14, 28]. The inter-cellular space in SC is usually less than 100 nm thick except at cell clusters junctions, in the 2 to 3 partly detached cellular layers close to skin surface (where corneocytes are less densely packed or even partially detached) and at the 2 to 3 layers at the bottom of SC where the terminal cells differentiation has only just begun [3].

In the model, the "mortar" represents the hydrophobic continuous matrix of lipids in which the corneocytes are embedded; this lipid matrix provides the only continuous diffusion pathway from the skin surface to the base of the SC [27, 37]. The

main lipids in the intercellular spaces of SC are ceramides, fatty acids, cholesterol, cholesterol sulphate and sterol/wax esters; unlike almost all other membranes in the body, the phospholipids in SC are largely absent. Ceramides are the largest group of lipids and its compact stacking is the primary determinant of the extremely stable physical properties of the SC [27]. According to Landmann model, the intercellular lipid matrix is generated by keratinocytes in the mid to upper part of the *Stratum Granulosum*, discharging their lamellar contents into the intercellular space [40]. In the initial layers of the SC, this extruded material rearranges to form broad intercellular lipid lamellae which then associate into multiple lipid bilayers, parallel to the surface of SC [31]. The hydrocarbon chains became arranged into regions of crystalline, lamellar gel and lamellar liquid crystal phases, thereby creating various domains within the lipid bilayers; it has been proposed that the distribution of crystalline and gel phases of the membrane lipids influences the diffusion of small molecules across the SC and into the dermis. [33, 38] Between the lipid bilayers, there are layers of water [28]. Water is an essential component, because it acts as a plasticizer to prevent cracking of the SC; some of extra water in maximally hydrated SC is sequestered into these layers, so-called “lacunae” [3, 31].

At the surface of SC, there is also an irregular and discontinuous layer (0.4–10 µm) consisting of sebum secreted by the sebaceous glands, along with sweat, bacteria and dead skin cells. However, this layer is considered to have a negligible effect as an additional barrier to permeation through the SC [14].

2.3.1.1.1. Transport Routes across the *Stratum Corneum*

Despite the composition and structure of the SC offers a main obstacle and a real challenge on drug delivery into and through the skin, its “brick and mortar” organization also provides some possible pathways to the passive diffusion of substances into the skin, as schematized in Figure 2-4. These pathways are through the keratinocytes (intracellular pathway), through the lipid matrix occupying the spaces between the keratinocytes (intercellular pathway) and across hair follicles, sebaceous

glands and sweat glands (transappendageal pathway) [14, 36]. However, the transport pathway is highly influenced by the structure, size and solubility of the penetrant [27]. Thus, understanding the physicochemical properties of the penetrant is essential to determine the predominant route of drug permeation and thereby optimize its delivery [31].

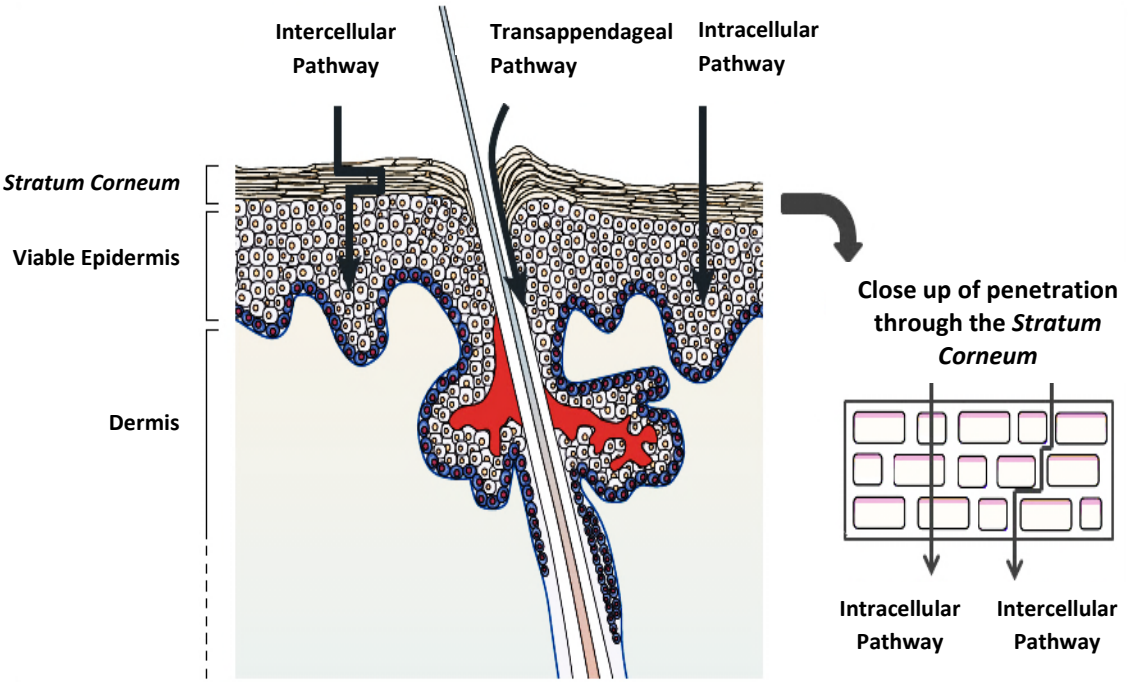

Figure 2-4: Routes for the penetration of substances through the *stratum corneum* (Adapted from Prausnitz M.R. *et al.*, 2004 [42]).

The major route of penetration for lipophilic molecules is through the lipid matrix [21]. Although this diffusional pathway (500 µm) is much longer than the simple thickness of the SC, it contains fluid lipids and channel-like structures, increasing the molecules insertion and migration through the intercellular lipid layers, providing higher diffusivity to them [3, 21, 41]. However, the intercellular space also contains hydrophilic domains which restrict the invasion of too lipophilic compounds. As a consequence, only substances with partition coefficients (logP) between 1 and 3 are well suited for skin absorption [21]. Finally, the size of penetrating species also

influences the absorption through this pathway, because penetrants need to fit into the intercellular space in order to move along it [21].

The hydrophilic entities have therefore, the propensity to cross normal skin within the aqueous regions near the outer surface of corneocytes or through corneocytes, along the most curved cell plasma membranes - intracellular pathway [3]. However, in this route, not only the drug must partition into and diffuse through the corneocyte but also, in order to move to the next corneocyte, the permeant must partioning into and diffuse through the lipid lamellae between corneocytes [31].

Until recently, the transappendageal pathway was barely considered as a penetration pathway because it covers only 0.1% of the skin surface area. Nevertheless, this route became to receive considerable attention once it provides an efficient penetration pathway and more important, it was realized that the appendages can act as reservoirs of topically applied substances [43, 44]. Among the appendages, the hair follicles (HFs) are of particular interest because they seem to be the preferential targets for nanoparticles [21, 43]. This favored penetration of nanoparticles through the HFs and their reservoir function for topically applied substances has the potential to revolutionize the treatment of hair follicle associated diseases (e.g., acne and some skin cancers) and the treatment of many diseases/disorders of human hair (e.g. hirsutism, graying, alopecia) that have dramatic effects on the appearance, socio-cultural status and self-esteem of the affected individuals [10, 45, 46].

2.4. The Follicular Pathway

Even though the HFs are increasingly recognized as a potentially route for the entrance of topical applied substances into the skin, the invasion of a substance into these structures is not an absorption process itself because, by definition, the compounds inside these appendages are still on the outside of the body [31]. However, since HFs are invaginations of the epidermis extending into the dermis, they provide a much greater actual area for absorption bellow the skin surface [47]. Also, as

it extend into the hair follicles, the surrounding SC layer is progressively reduced, which may lead to a faster and more efficient diffusion of solutes from out of the follicles to the inside of the skin; the dense network of blood capillaries at the lower levels of the HFs also facilitates the uptake of topically applied substances [14, 31]. Another feature of the HFs that makes them interesting for topical delivery is their reservoir function [41]. While the reservoir of the SC is located in the uppermost cell layers of the horny layer (approximately 5 µm), the reservoir of the HFs is usually extended deep in the tissue up to 2000 µm [48].

Even if the HFs are potential routes for the absorption of topically applied substances, not all hair follicles are available for penetration and they have to be distinguished between "open" and "closed" [49]. The hair follicles "open" to penetration exhibit hair growth and/or sebum production which act as a pumping system, pushing topically applied substances mechanically into the hair follicles when the hairs are in motion [50]. This was kind of surprising as the direction of hair growth and sebum flow are opposed to the invasion of materials into the follicles, suggesting an "active" uptake mechanism transporting them deep into the follicle [48]. In the "open" hair follicles, the release of sebum also influences the absorption and, since sebum consist mostly neutral, non-polar lipids, it provides a lipoidal pathway that it will favor the penetration of more lipophilic permeants [26, 47]. Depending on the skin samples, approximately 50-70% of hair follicles are open for penetration [36].

2.4.1. Anatomy of the Hair Follicles

In order to develop appropriated studies of follicular delivery, an understanding of the structure of the HFs is useful. The hair follicle, represented in Figure 2-5, is composed of a hair bulb and a hair shaft [46, 47]. The hair bulb, localized at the base of the hair follicle, encloses a small papilla of dermis, which it is a structure of actively growing cells that produce the long fine cylinder of a hair [51]. The dermal papilla is connected to the blood vessels, an important feature when the HFs are used as route for transport of drugs into the systemic circulation [47, 52]. The hair bulb and

shaft are enveloped in an inner root sheath and an outer root sheath [52]. The outer root sheath is a stratified epithelium that is continuous with the epidermis and this continuity is responsible for the increased surface area of absorption beneath the surface of the skin, making of this layer the most important with regard to drug delivery [47]. On the contrary to the outer root sheath, the inner root sheath ends about halfway up the follicle [46].

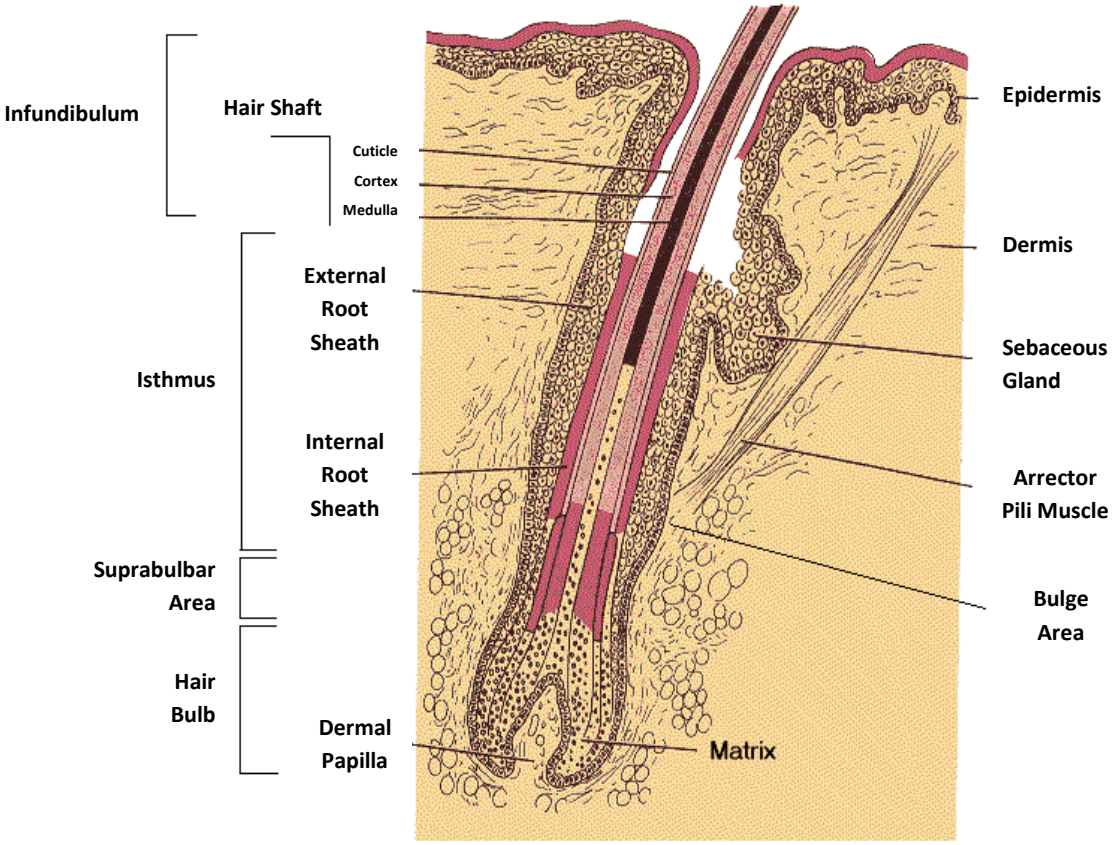

Figure 2-5: Cross-section diagram of a human hair follicle (Adapted from Meidan V.M. *et al.*, 2005 [46]).

As it can be seen in the figure above, the hair follicle is associated through ducts (in the upper part of the follicle canal) with sebaceous glands that are responsible for the production of sebum and their release into the follicular canal [46, 47]. Connected to the hair follicle is also an adjoining arrector pili muscle. The whole structure, comprising the hair follicle, sebaceous glands and adjoining arrector pili

muscle, is called pilosebaceous unit; usually, the terms hair follicle and pilosebaceous unit are used interchangeably [52].

The hair follicle (or pilosebaceous unit) can be divided into four parts: the infundibulum (zone between the skin surface and the point where the sebaceous gland duct opening into the follicle canal), the isthmus (between the sebaceous gland duct opening and the bulge region), the suprabulbar zone (between the bulge area and the hair bulb) and the hair bulb. The lower part of the infundibulum, called infrainfundibulum, may experience a continuous loss of epidermal differentiation occurring towards the isthmus and creating the major entry point for applied substances [52]. As the hair follicles are composed of many structures and have several zones with different populations of cells, they offer a lot of therapeutic targets for the treatment of disorders of human hair and hair follicle associated diseases [53].

2.4.1.1. Target Structures for Follicular Therapy

At the HFs, the major target areas for drug delivery are the sebaceous glands, the bulge region and the hair bulb (Figure 2-5) [54]. The sebaceous glands represent an important therapeutic site because they are implicated in the aetiology of androgenetic alopecia (with the clinical consequence of increased hair loss) and acne, as well as other sebaceous gland dysfunctions [10, 49]. Along with the sebaceous glands, the bulge region is the most important target site within the hair follicle. Since the bulge region is the host of epithelial stem cells with high proliferative capacity and multipotency (which make them capable to repopulate hair follicles, sebaceous glands and epidermis), it opened new directions for their utilization in hair and skin regenerative medicine [10]. The gene delivery to stem cells of the bulge region can facilitate long-term gene correction of congenital hair disorders (hair loss or hair overgrowth) or genetic skin disorders; however, for this purpose, profound knowledge of genes and signaling pathways involved in hair diseases are necessary, in order to allow specific modulation using, for example, RNA interference [10, 49, 52]. The localization of melanocytes stem cells at this region also offers the opportunity to treat

pigmentation disorders [47]. Another desirable target in hair follicle is the hair bulb, where matrix cells and melanocytes can be found [11]. Such as epithelial and melanocyte stem cells of hair bulge, the hair matrix cells and melanocytes (involved in the production of melanin through melanogenesis) of hair bulb are also responsible for follicle reconstitution (playing an important role in the control of hair growth) and pigmentation, respectively [10, 52].

2.5. Nanoparticles for Hair Follicle Therapy

As mentioned before, when applied topically, nanoparticles have tendency to accumulate preferentially in the hair follicle orifices (see section about "Transport Routes across the *Stratum Corneum"*); on the other hand, free drugs can enter the skin through the *stratum corneum* and the hair follicles, indistinctly. When the hair therapy is intended, the loading of therapeutic agents into nanoparticles is important because it reduces the penetration of drugs through the trans-epidermal pathway, increasing their concentration in the hair follicle [31]. The use of nanoparticles for hair therapy is also favorable because, it is known that drugs penetrate better into hair follicles when they are inside the particles [49]. However, the penetration of nanoparticles within the follicular duct is dependent of their diameter, with smaller particles showing increased penetration depths [11]. This particularity is also significant for hair therapy, since the targets for drug delivery are found at different depths of the follicle (Figure 2-5). Thus, it is possible to reach a specific site of action (located at a certain depth) by controlling the size of the applied particles [52]. Once inside the follicles, the storage time of nanoparticles is longer, when compared to short-time storage in SC. This happens because the depletion of stored nanoparticles from follicular reservoir is dependent of slow processes as penetration of particles into deeper tissue layers or by their release with the outflow of sebum [36, 55]. The long time storage of nanoparticles within the follicle canal ensures a prolonged drug release, which enables the reduction of the applied dose as well as the frequency of application [31].

Since the follicular pathway favors the penetration of lipophilic rather than hydrophilic drug carriers (see section about “The Follicular Pathway”), many kinds of lipophilic particles have been investigated for follicular target and drug delivery upon topical application [45, 52]. Among them, lipophilic polymeric nanoparticles are the most promising technology and they have shown many advantages over other systems. Polymeric particles helps to mask the intrinsic properties of encapsulated drugs, which can facilitate the entrance of therapeutic agents that otherwise have low solubility on the sebum (e.g., hydrophilic substances) [22, 37].

2.5.1. Polymeric Nanoparticles

Polymeric nanoparticles can be synthetized from synthetic and natural polymers, varying in polarity from hydrophilic to hydrophobic [56]. However, natural polymers as proteins and polysaccharides are not extensively used because they vary in purity and often require preparation processes that can lead to drug degradation [37]. Concerning to the synthetic ones, the accumulation and the potential cytotoxicity of non-biodegradable polymers is a major problem and limits their use in humans. Therefore, just a few types of biocompatible and biodegradable polyesters like poly (lactic acid) (PLA), poly lactic-co-glycolic acid (PLGA) and poly-ε-caprolactone (PCL) have been widely studied [11, 57]. Among these polyesters, in the preparation of polymeric drug delivery systems for long-term sustained-release of various drugs, PLA has numerous advantages over the others because, it is produced from renewable resources, it is recyclable and compostable, its physical and mechanical properties can be easily altered though the manipulation of its architecture and it is approved by Food and Drug Administration (FDA) for clinic use [58, 59].

PLA (Figure 2-6) is a linear, lipophilic, thermoplastic, high-strength and high-modulus polymer, soluble in organic solvents but insoluble in common alcohols and water [11, 18, 60]. Its constituting monomer is lactic acid, obtained annually from renewable resources such as corn starch or sugarcane, by carbohydrate fermentation [11, 60]. Lactic acid exists in two optically active configurations, L- lactic acid and D-

lactic acid and, polymers synthesized from one of them are partially crystalline while the racemic poly (D, L-lactic acid) is amorphous [18].

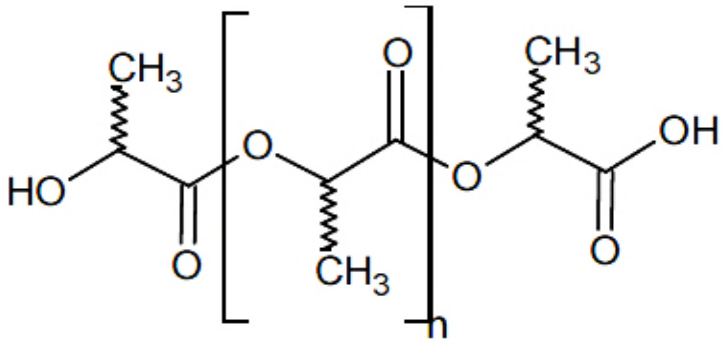

Figure 2-6: Chain structure of PLA (Online image, available at http://www.medicinescomplete.com/mc/excipients/current/images/Ecpoly_dl_lactic_acidC001_default.png; accessed on September 10, 2012).

The synthesis of PLA can follow two different routes of polymerization: condensation/coupling and ring-open polymerization [60]. The first route leads to the formation of a polymer by the linking of monomers with the release of water or similar simple substances, allowing the production of low molecular weight PLAs (< 3000 g/mol). On the other hand, ring-opening polymerization produces polymers with higher molecular weights and the method is based in addition polymerization where the terminal end of a polymer acts as a reactive center and cyclic monomers join to form a larger polymer chain [18, 59].

The presence of ester linkages in the polymer backbone allows its hydrolytic degradation in aqueous environment. The degradation rate is dependent on several parameters such as crystallinity (crystalline PLA degrades slower), molecular weight (low molecular weight PLAs degrade faster) and the environment conditions (pH, ionic strength, temperature) [18]. Regarding to the production of drug delivery systems, these dependence between the properties of polymer and its degradation rate is an important advantage of PLA; since the degradation rate is related to the release of

drugs, altering the polymeric material, it is possible to manufacture systems with a rate delivery that can be modulated depending on duration of the desired effect [61]. Following the hydrolysis of the polymer, the only degradation product is lactic acid, which it is biocompatible, metabolized through citric acid cycle and then removed from the body [18].

2.5.1.1. Preparation of Drug-loaded Polymeric Nanoparticles

Numerous methods such as single emulsion [62], spontaneous emulsion solvent diffusion (SESD) [63], double emulsion [23], salting-out [64], spray drying [65] and nanoprecipitation [66] have been proposed for the preparation of polymeric drug-loaded nanoparticles. All of these methods are able to produce NPs with high yield and high encapsulation efficiency and, in general, the process is critical in determining nanoparticle size [67, 68]. Considering the encapsulation mechanism, the drugs can be entrapped, dispersed, dissolved within or simply adsorbed on the matrix of nanoparticles (Figure 2-7), depending upon the method of preparation and the physico-chemical properties of the therapeutic agent [22].

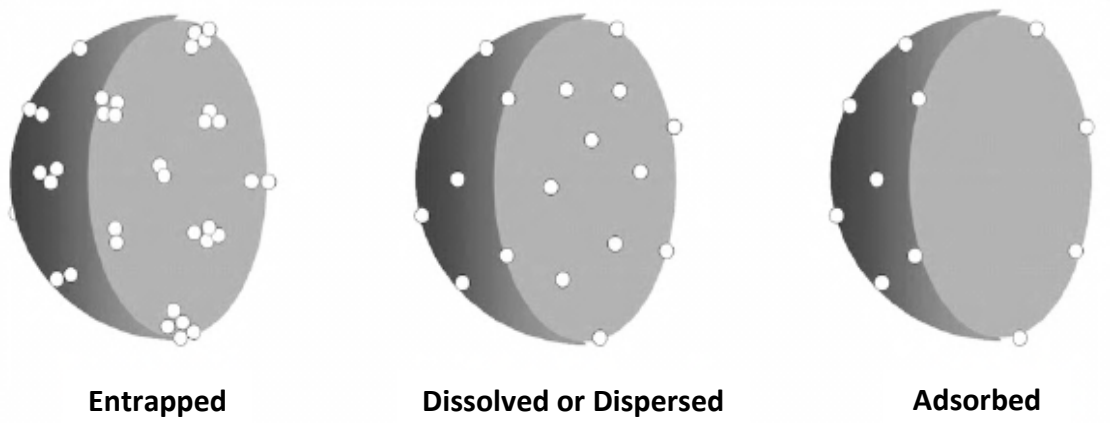

Figure 2-7: Mechanisms of drug encapsulation on the nanoparticles (Adapted from Guterres S.S. *et al.*, 2007 [22]).

The great challenge in choosing a method for the preparation of particles consists on an adequate formulation, establishing the ideal amounts of drug, polymer, solvent and non-solvent, which it will allow the production of stable nanoparticles, efficient entrapment of drugs and their release according to the desirable profile [15, 67].

In the production of polymeric particles with single emulsion method (also known as solvent evaporation method), Figure 2-8, the polymer is dissolved in an organic solvent along with the drug and this mixture is emulsified into an aqueous solution, using a surfactant/emulsifying agent. After formation of stable oil in water (o/w) emulsion, the organic solvent is evaporated from dispersed oil droplets (containing both polymer and drug) [62].

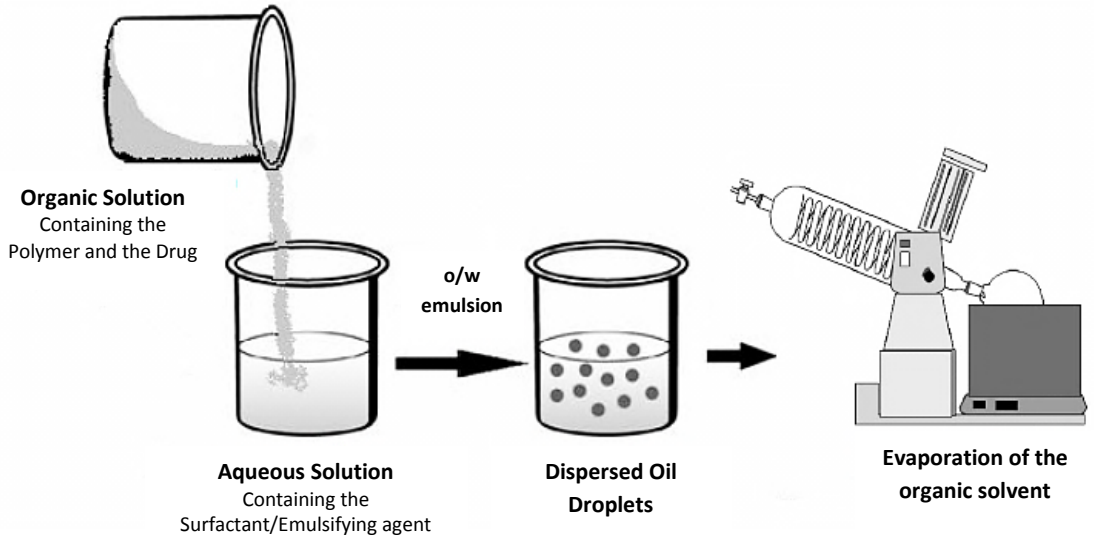

Figure 2-8: Production of polymeric particles with single emulsion method (Adapted from Gomes V.M.A., 2009 [15]).

The spontaneous emulsion solvent diffusion technique is a modified version of the solvent evaporation method, schematized in Figure 2-8 [63]. In this method, the organic solution used to solubilize the polymer and the drug is a binary mixture of a water-miscible organic solvent and a water-immiscible solvent. The polymeric solution is then poured, with mechanical stirring, into an aqueous phase containing a stabilizer

and emulsion droplets are formed; droplets can also be induced by sonication and homogenization [57, 69]. Due to the quickly spontaneous diffusion of water-soluble solvent out from each emulsion, an interfacial turbulence between the two phases is created and a drastically reduction in the size of particles is obtained (Figure 2-9) [15, 62]. The consequent removal of the organic solvent from the system makes the droplets solidify to finally form polymeric nanoparticles varying in size from 100 to 400 nm. However, a major concern about this method is the large-scale production that sometimes causes a severe aggregation in the particle formation when the polymeric concentration is increased to an acceptable range for industrial purposes [57].

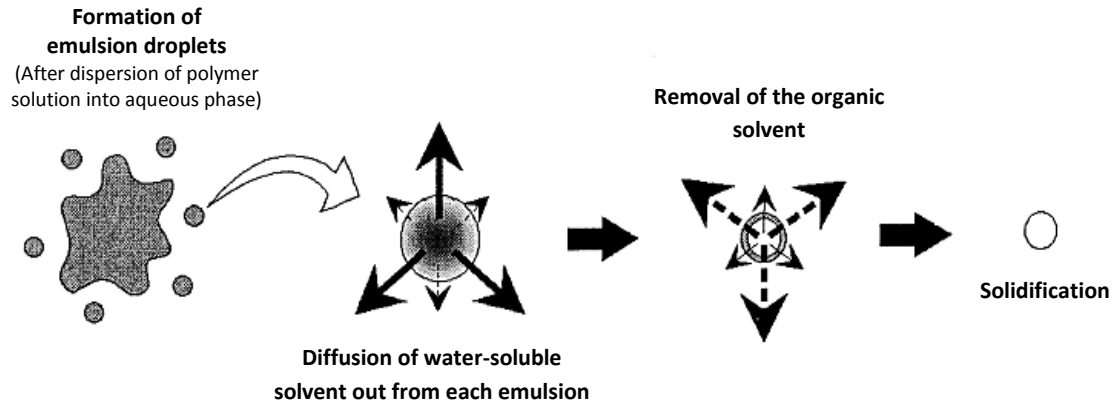

Figure 2-9: Mechanism of nanoparticles formation by the SESD method (Adapted from Murakami H. *et al.*, 1999 [57]).

The SESD method and solvent evaporation previous described are widely used for the encapsulation of hydrophobic drugs but they have poor results incorporating bioactive agents of a hydrophilic nature. Hydrophilic drugs have a high tendency to move from the organic phase to the outer aqueous phase, not into the polymeric nanoparticles [67, 69]. Thus, another emulsification method - the double emulsion technique, represented in Figure 2-10 - has become the favored protocol for the encapsulation of this kind of compounds [23]. First, the drug for encapsulation is dissolved in water and this phase is dispersed in an organic solvent, which it contains

the degradable polymer - the first emulsion, water in oil (w/o), is formed. Then, the w/o emulsion is dispersed into an aqueous medium (containing a stabilizer), forming the final w/o/w emulsion. Once again, as the solvent evaporates, the polymer hardens encapsulating the drug [16].

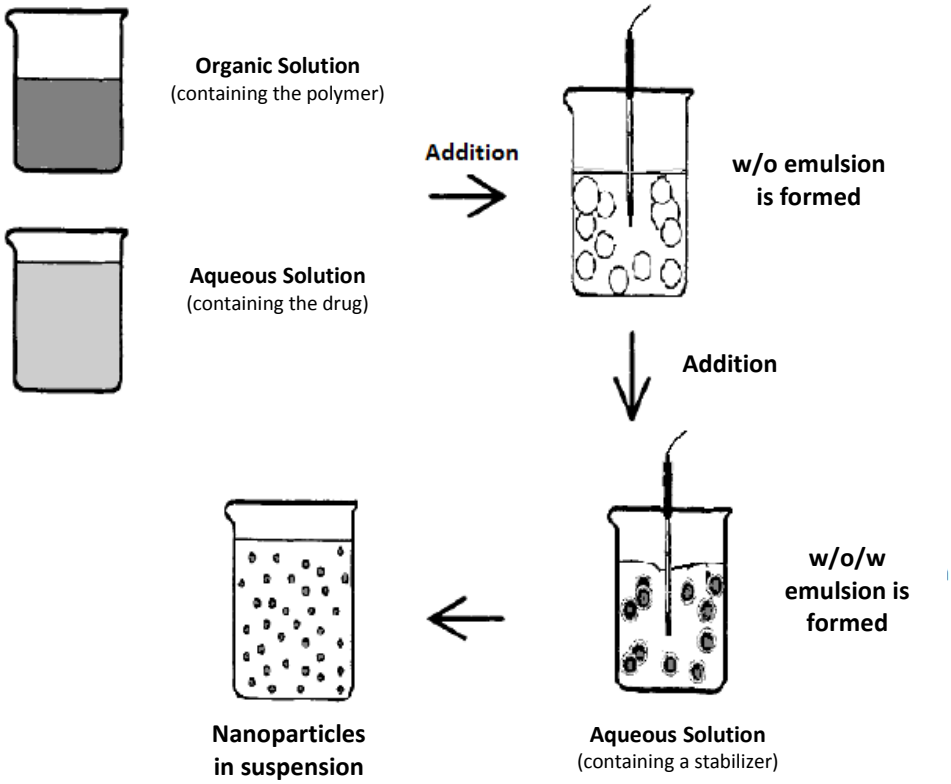

Figure 2-10: Method for the preparation of nanoparticles based on a double-emulsion (Adapted from Gomes V.M.A., 2009 [15]).

Another method to prepare polymeric nanoparticles is the salting-out process [64]. Using this technique, a w/o emulsion is formed containing the polymer, acetone, magnesium acetate tetrahydrate, stabilizer, and the active compound. Subsequently, water is added until the volume is sufficient to allow the diffusion of the acetone into the water, which results in the formation of nanoparticles. This suspension is purified by cross-flow filtration and lyophilization. One disadvantage of this procedure is that it uses salts that are incompatible with many bioactive compounds [69].

A preparation technique that it is suitable for industrial scalable processing is spray drying because it is very rapid and convenient, also having very few processing parameters. In this process, drug-loaded particles are prepared by spraying a solid-in-oil dispersion or water-in-oil emulsion in a stream of heated air. The type of drug (hydrophobic or hydrophilic) decides the choice of solvent to be used in the process [65].

The nanoprecipitation, first introduced by Fessi *et al.*, is the most commonly used technique to formulate polymeric nanoparticles, intended for cutaneous applications [22, 66]. It is a simple, fast, efficient, economic and reproducible method for the preparation of small particles, based on precipitation and subsequent solidification of the polymer at the interface of a solvent and a non-solvent (Figure 2-11). Thus, the process is often called solvent displacement or interfacial deposition. [18, 22, 68] The choice of the polymer, solvent and non-solvent system is critical for the success of the method and the nature of the polymer-solvent interactions has been reported to affect the properties of the nanoparticle preparation. However, no clear guidelines about the influence of each of the three components of the system have yet emerged [68].

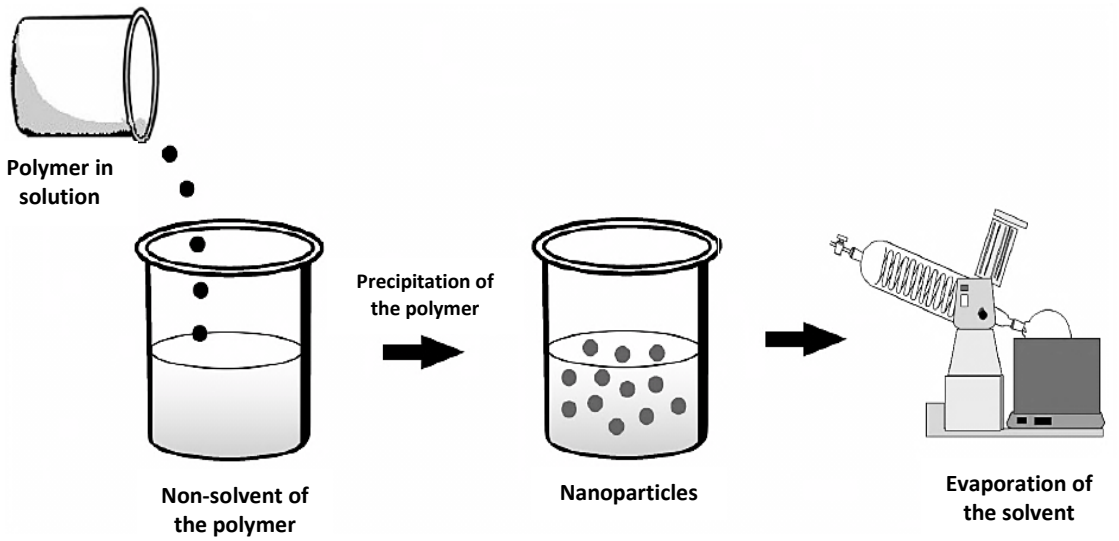

Figure 2-11: Schematic illustration of the nanoprecipitation method (Adapted from Gomes V.M.A., 2009 [15]).

To achieve nanoprecipitation, the polymer is dissolved in an organic solvent (or mixture of solvents) and added to a non-solvent of the polymer wherewith the organic solvent is miscible; depending on its solubility, the drug to be encapsulated must be dispersed in the aqueous solution or dissolved in the organic solvent before the fusion of the phases [18, 68]. The nanoparticles form instantaneously by precipitation of the polymer and Marangoni effect is considered to explain the process: solvent flow, diffusion and surface tension at the interface of the organic solvent and the aqueous phase cause turbulences, which form small droplets containing the polymer; subsequently, as the solvent diffuses out from the droplets, the polymer precipitates. To finish, the organic solvent is typically removed by evaporation [18, 68]. Although the presence of surfactants/stabilizers is not indispensable for the formation of the particles, they can be included in the process to modify the size and the surface properties or to ensure the stability of the nanoparticle dispersion (especially during the early stages of the precipitation). Thus, in this method, no emulsification step (which is usually part of a nanoparticle preparation process), laborious processing conditions or special laboratory ware is needed and the nanoparticles prepared by nanoprecipitation are typically smaller than 500 nm [18]. Nevertheless, this technique suffers the drawback of a poor encapsulation efficacy of water-soluble drugs due to the rapid migration, and therefore loss of drug, into the aqueous phase [70].

The methods previously mentioned can be successfully employed for the encapsulation of many drugs as hinokitinol [71], minoxidil [72], latanoprost [73], finasteride [74], cyclosporine A [75] and tamoxifen [76]. All of these therapeutic agents have been studied and developed for the safe and effective treatment of several hair follicle disorders/diseases.

2.5.1.2. Drug Release from Polymeric Nanoparticles

After the penetration of nanoparticles inside the hair follicle canal, the encapsulated drug is released and, independently, it penetrates through the intact

barrier of the hair follicle to reach the target structure (Figure 2-12) [50]. The rate of release is dependent upon desorption of the surface-bound/adsorbed drug, diffusion of drug through the polymer wall, nanoparticle matrix degradation or a combined degradation/diffusion process [62]. In nanoparticulate DSS, the ideal release profile of a therapeutic agent is a near zero-order profile, which establishes a more constant flow of the bioactive agent out of the carrier, maintaining more appropriate steady level of the drug at the site of delivery [13]. In the development of a drug carrier, in order to achieve this steady release rate, it is important to know the properties of the delivery system, the characteristics of the drug and the degree of polymer-drug interaction because they can influence the release of the bioactive compound [23].

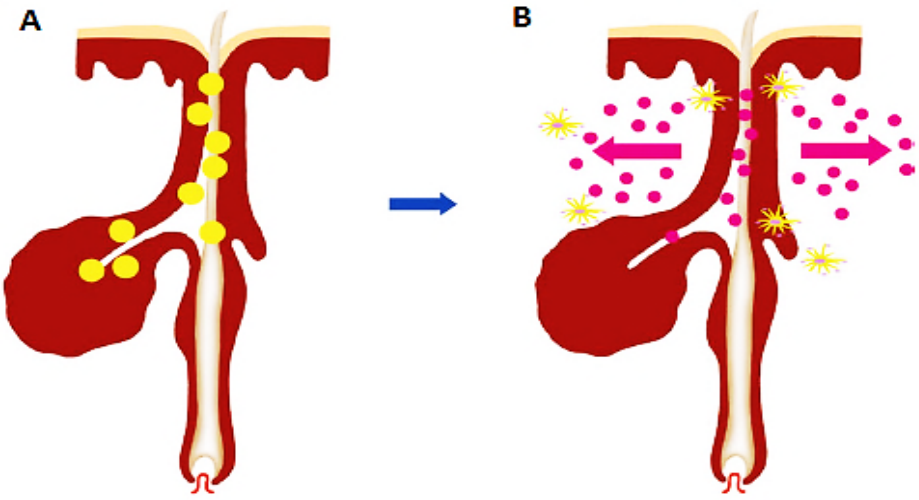

Figure 2-12: Release of the drug and targeting of follicular structures. A) Accumulation of polymeric drug-loaded nanoparticles within the hair follicle canal, at the level of the target structure. B) Release of the drug from the particles and its penetration through the hair follicle barrier. (Adapted from Papakostas D. *et al.*, 2011 [11]).

Regarding to the properties of the carrier, a decrease in particle size (and increase in the surface area) results in high release. Higher porosity, inducing a larger inner surface, can increase the influx of the release medium into the particles and, thereby, also facilitate the drug diffusion rate. In addition, specific properties of the

polymer that constitutes the matrix, as crystallinity and molecular weight, can also affect the release of the drug [77]. Polymers with more crystallinity have limited flexibility since the ordered alignment of the polymer chains lower the free volume. Thus, they form particle cores with high microviscosity that prevent the diffusion of the drug and water molecules. In contrast, amorphous polymers tend to form cores with lower microviscosity and a higher rate of diffusion [23]. Polymer with higher molecular weight have lower degradation rates, because it requires more time to degrade longer polymer chains than small polymer chains, and the release of drugs is slower [65].

Concerning to the characteristics of the encapsulated drug, the amount of it present in the particles influence the drug release kinetic and usually, an increasing in the drug loading results in an increased rate of drug release. Conversely, an increase in the molecular volume and molecular weight of the drug lead to a lower diffusion coefficient and consequently, a lower release rate [23]. The entrapment of some molecules as amines can interfere in the degradation mechanism of hydroxy acids polymers (e.g., PLA), affecting the release rate [61].

Finally, the degree of polymer-drug compatibility also influences the rate of drug release from the particles. When drugs are miscible with the polymer, and consequently possesses good polymer-drug compatibility, there is an increase in the extent of interaction between them that can slower the release of the drug [23].

2.6. Safety Aspects of Nanoparticles

Considering the enormous potential of nanotechnology-related products and the prospect of mass commercialization in the coming years, namely for cosmetic application, there is considerable concern regarding to the safety of manufactured nanomaterials, as they may have characteristics different from their large-scale counterparts [11, 17]. Accordingly, the risk assessments developed for ordinary materials may be of limited use in determining the health and environmental risks of nanotechnology products [17].

Nanoparticles, because of their size, can get to places in the environment and human body that are inaccessible to larger particles, and unusual or unexpected exposures can occur. Since these particles also have larger surface-area-to-mass ratio than bigger materials of the same composition and, as biological/chemical reactions typically take place at the surface of materials, it has been hypothesized that nanoparticles will be more reactive than bulk materials, undergoing dynamic interactions with components of the environment with which they are in contact [17]. While this increased reactivity can be a useful attribute for nanomaterials, it also carries potential risks and research looking into both particle-associated effects on living organisms and particle alterations in their physico-chemical properties as a result of particle-tissue interaction (which affect its behavior) is crucial and it must be considered in conducting a risk assessment related to both human health and environmental safety [11, 17].

Regarding to cosmetic applications, concerns have been raised about the potential danger which may occur as a consequence of nanoparticle contact with human skin. Thus, an advanced research is required to understand the behavior of nanomaterials, including whether the nanoparticles remain on the surface of the skin and/or in the outer dead layer (*stratum corneum*), the mechanism by which they penetrate intact skin and how far a particle can penetrate the skin. For these studies, it is important to know the physico-chemical characteristics of nanoparticles as size, surface charge, specific surface area, porosity, water solubility, photocatalytic activity and the potential for free radical formation. An understanding of how these properties might affect the ability of nanoparticle to penetrate the skin would permit the engineering of the nanomaterial to prevent it from either affecting skin cells or possibly passing into the dermis and gaining access to the bloodstream [17].

About the toxicity of the nanoparticles for follicular targeting, these carriers seems to be safe since they are mostly made of biodegradable and biocompatible materials. Also, as long as their dimensions are larger than 100 nm, they are not able to translocate into the viable epidermis of intact skin and, after some time (next to the release of the bioactive agent) they are moved out of follicles because of sebum production and excretion [45, 52]. However, there are still scarcely any studies focused

on the long term fate of nanoparticles in the hair follicles, and this aspect definitely needs investigation [52].

3. MATERIALS AND METHODS

3.1. Materials and Equipment

3.1.1. Chemicals and Solvents

The chemical reagents used in this work were Poly (D,L-Lactic Acid) with a molecular weight of 18000-24000 Da, Pluronic F68 (a non-ionic surface-active block co-polymer also known as Poloxamer 188), Nile Red (318.4 Da, HPLC grade, purity ≥ 98%), Fluorescein 5(6)-isothiocyanate (398.4 Da, HPLC grade, approximately 90%), Methanol (ACS reagent grade, ≥ 99.8%) and Isopropyl Myristate (Kosher grade, ≥ 98%). All of these chemicals were purchased from Sigma-Aldrich (Sigma Chemical Co., St. Louis, MO). Acetone and Ethanol were of the highest grade commercially available and purchase from several suppliers.

The storage of the reagents was done following the instructions of the manufacturers and they were handled according to practices consistent with their security information.

3.1.2. Porcine Skin Tissue

Full-thickness porcine skin (abdomen region) was obtained from Central Carnes – Matadouro Central de Entre Douro e Minho, Lda. (Lousado, Portugal); skin samples were excised on-site from freshly slaughtered pigs. The collection at the slaughterhouse, as well as the handling of porcine skin tissue for purposes related to scientific research, was approved by DGV-Direção Geral de Veterinária.

3.1.3. Equipment

Equipment used throughout the experimental work, their suppliers and the methods associated with them are summarized in Table 3-1.

Table 3-1: List of equipment, used in the course of this experimental work.

Equipment	Method
20 kHz Vibracell™ CV 33 – Probe type ultrasound source fitted with a 3 mm diameter titanium micro-tip (Sonics and Materials Inc., CT, USA)	Sonication
EmulsiFlex-C3 (Avestin, Ottawa, Canada)	High Pressure Homogenization
ZetaSizer Nano ZS with ZetaSizer 6.01 software (Malvern Instruments Ltd, Worcestershire, UK)	Photon Correlation Spectroscopy (PCS); Laser Doppler Anemometry (LDA)
NOVA™ Nano SEM 200 (FEI™, OR, USA)	Scanning Transmission Electron Microscopy (STEM)
SynergyMx with Gen5™ Microplate Data Collector and Analysis Software (Bio-Tek® Instruments, Inc., VT, USA)	UV-Vis Spectrophotometry
Diffusion Cell System V3A-02 (PermeGear Inc., PA, USA)	*In vitro* Follicular Penetration Studies
Leica CM1900 cryostat (Leica Microsystems, Numsloch, Germany)	Cryosectioning
Leica DM 5000B Microscope with DCF350FX Camera and AF6000 Modular Systems (Leica Microsystems Numsloch, Germany)	Fluorescence Microscopy

3.2. Methods

3.2.1. Preparation of PLA Nanoparticles

PLA nanoparticles were prepared based on the nanoprecipitation method (also known as solvent displacement technique), originally described by Fessi *et al*. As reported by these authors, the polymer was dissolved in an organic phase, acetone - 2% (w/w), and further added to an aqueous phase containing Pluronic F68. The aqueous phase immediately turned milky with bluish opalescence due to the polymer precipitation in the form of nanoparticles. The concentration of the surfactant in the resultant solution was 0.6% (w/w) and the organic phase to aqueous phase ratio was 1:2. Finally, the solvent was completely removed under reduced pressure at 25 °C with a rotary evaporator. The nanoparticles suspensions in water were stored in a refrigerator at 4 °C. [66]

To promote the production of nanoparticles with desirable sizes for follicle targeting, some alterations were introduced to the original method of nanoprecipitation, according to three different techniques: agitation, sonication and homogenization. In the first technique, the organic phase was added drop wise (at a uniform rate) into the aqueous phase with stirring at 100 rpm and the solution obtained was stirred overnight at the same velocity. For sonication, after the addition of the organic phase to the aqueous phase, the preparation was submitted to an ultrasound treatment. The reaction vessel was an open glass cell (diameter of 19 mm and height 75 mm) which contained 15 mL of sample solution and its temperature was maintained at 5 ± 1 °C. The probe was placed in the anti-nodal point (19 mm depth) and the power delivery was controlled as percentage amplitude at 40%. Two times of sonication were tested (15 and 18 min), with a pulsed duty cycle of 8 s on, 2 s off in order to determinate which time promotes the production of nanoparticles with most appropriates sizes attending to the objective of the particles. Finally, in homogenization, the acetonic solution of PLA was added to aqueous phase and the resultant solution was homogenized for 18 min, with a constant flux of 40 mL/min.

3.2.1.1. Addition of a Non-Solvent to the Solvent Phase

Since the presence of a portion of a non-solvent for the polymer, in the solvent phase, can improve the properties of the particles, the effect of different ratios of ethanol and water were tested in the production of PLA nanoparticles [66]. Initially, to evaluate the affinity of PLA to ethanol and water, the cloud points were determined applying the titration technique. Acetonic solutions containing different concentrations of PLA were slowly titrated with ethanol or water until the polymer begins to precipitate, noted by the appearance of a distinct cloudiness – the cloud point. The percentage of the non-solvents necessary to reach the cloud point is considered the maximum fraction of non-solvent in the mixture with acetone to continue to be complete dissolution of the polymer [78]. For a PLA concentration of 2% (w/w), the maximum proportion of ethanol in the mixture with acetone is 55% and for water is just 10%. With the results of titrations, PLA nanoparticles were produced, according to the techniques previously described, using mixtures of Acetone/Ethanol (45/55, v/v) and Acetone/Water (90/10, v/v) to dissolve the polymer.

3.2.1.2. Effect of the Concentration of Pluronic F68

The effect of the concentration of the surfactant agent, in the properties of the particles, it was also evaluated. Thus, solutions of 2% (w/w) of PLA were prepared and added to aqueous phases containing different amounts of Pluronic F68; the concentration of the surfactant agent in the resultant solutions was 0.6% (w/w), 1% (w/w), 1,5% (w/w) and 2% (w/w).

3.2.2. Yield of Nanoparticles

Not all of the polymer used in the preparations (m_{total}) can form nanoparticles since there is some starting-material that aggregates during the nanoprecipitation

process (m_{agg}). Thus, the yield of nanoparticles can be determined according to the Equation 3-1.

$$Yield\ of\ Nanoparticles\ (\%) = \frac{m_{total} - m_{agg}}{m_{total}} \times 100$$

Equation 3-1: Determination of efficiency of nanoparticles formation.

For the calculation of the mass of aggregates, it was considered all of the polymeric fractions which were not nanoparticles - polymer stuck to the magnetic stirrer, to the flask or to other recipients which contained the formulations (polymer losses) and particles in the range of micrometers or above [68].

In the quantification of polymer losses, all the materials that contained or were in contact with formulations were washed with acetone to dissolve the polymer stuck to them and this solution was further recovered. Then, excess of methanol was added to precipitate the polymer and the solvents were removed with rotary evaporator. The recovered polymer was dried and weighted [68].

To determine the mass of produced particles that lies above the range of nano sizes, the formulations were passed through a GF/C glass microfiber filter with pore size of 1.2 µm (Whatman, Maidstone, UK). The recovered polymer in the filters was dried and weighted [58].

3.2.2.1. Effect of Ethanol in the Yield of Nanoparticles

To evaluate the effect of ethanol, used together with acetone to dissolve the polymer, in the yield of nanoparticles, the particles were prepared by using different ratios of Acetone/Ethanol – 55/45, 50/50 and 45/55%. The formulations were prepared as previously described and the yield was determined following the methodology described above. Since the fraction of ethanol could also promotes alterations on the nanoparticles properties, the size, Polydispersity Index (PDI) and zeta (ζ)-potential of the produced particles were also investigated.

3.2.3. Characterization of the Particles

The size, PDI and ζ -potential of nanoparticles were determined using ZetaSizer Nano ZS equipment; all the measurements were performed at 25 ± 1 °C. Each value is the average of at least three independent measurements and the results were expressed as mean value ± standard deviation.

The morphology of the particles was also assessed, using Scanning Transmission Electron Microscopy (STEM).

3.2.3.1. Particle Size and Size Distribution Measurements

The size and PDI of the particles produced above were determined by Photon Correlation Spectroscopy (PCS). This method measures the Brownian motion of the particles, which allows the determination of its diffusion coefficient. The Stokes - Einstein equation (Equation 3-2) relates the diffusion coefficient (D) with the diameter of the particles (d), also using the values of Boltzman constant (K) and temperature in Kelvin (T). PDI is indicative of the heterogeneity of the sample size and its values ranges between 0.0 and 1.0 – the higher the PDI, the greater the heterogeneity of the sample.

$$D = \frac{KT}{3\pi d}$$

Equation 3-2: Equation of Stokes-Einstein used to determinate the diameter of the particles.

3.2.3.2. Analysis of the Zeta-Potential

Zeta-Potential is a characteristic parameter of the nanoparticles charge, since the surface potential cannot be directly measured. For its determination, the particles

are submitted to a weak electric field and their electrophoretic mobility is determined by laser Doppler anemometry (LDA). With Henry equation (Equation 3-3), it is possible to relate the electrophoretic mobility (μ_e) with Zeta-Potential (ζ-potential). The values of dielectric constant (ε), viscosity of the medium (η) and f(Ka) - role of Henry - are also present in the equation.

$$\mu_e = \frac{2\varepsilon\zeta - \text{potential}f(\text{Ka})}{3\eta}$$

Equation 3-3: Equation of Henry used to determinate the electrophoretic mobility of the particles.

3.2.3.3. Morphology of Nanoparticles

The shape and surface morphology of nanoparticles were analyzed by STEM, which allows the direct observation of nanoparticles suspended in a liquid layer. The solution containing nanoparticles were diluted and placed onto copper grids with carbon film 400 meshes, 3 mm diameter. Then, the observations were performed at 15 kV using a NOVA Nano SEM 200 FEI [20].

3.2.4. Preparation of Dye-loaded Nanoparticles

Fluorescent particles containing Nile Red (NR) or Fluorescein 5(6)-isothiocyanate (FITC) were prepared – these fluorochromes were used as models of lipophilic (NR) and hydrophilic (FITC) compounds. NR was chosen because of its emission in the red region of the light spectrum, where skin has a low auto-fluorescence. FITC was chosen because of its excellent fluorescence quantum yield.

The particles were obtained employing the same techniques used to produce empty particles, with the dye being dissolved along with the polymer. The solution containing PLA and the dye was added to the aqueous phase and the concentration of

dye in the resultant solution was 0.3% (w/v). Then, the solvents were evaporated and the size, PDI and ζ-potential of the particles were measured. During the entire experimental procedure, the solutions were protected from the light [45].

3.2.4.1. Determination of Entrapment Efficiency

The amount of the compounds, which were not entrapped in the nanoparticles, was determined with Ultraviolet (UV)-Spectrophotometry. Two fractions were considered for this quantification: the amount of dye entrapped in the aggregates of polymer that remains stuck to the material (see section about "Yield of Nanoparticles") and the dye that was not entrapped inside nanoparticles and remained free in the formulation.

For the quantification of the dye in the aggregates, after the preparation of nanoparticles, all the materials that contained or were in contact with formulations were washed with acetone to dissolve the polymer and the dye stuck to them. An aliquot of this solution was diluted with the adequate solvent and the fluorescence intensity was measured spectrophotometrically. For Nile Red, the dilution was made in acetone and measurements were performed with an excitation wavelength of 536 nm and emission wavelength of 608 nm [79]. For FITC, the dilution was made in water and the wavelengths of excitation and emission were 495 nm and 525 nm, respectively.

The amount of free dye was achieved with dialysis. The formulations with particles containing the dyes were placed in dialysis membranes (molecular weight cutoff 12400 Da) and dialyzed against distillated water for 24h. After that, the dialysis medium was changed two times at each 2h. Aliquots of the dialysis mediums were collected and diluted in distillated water and the fluorescence of the samples was measured; for Nile Red the excitation and emission were performed at 591 nm and 657 nm, respectively [79]. However, for FITC it was used the same wavelengths previously mentioned for the quantification of the dye in the aggregates.

As empty PLA-NPs and Pluronic F68 showed no fluorescence for the wavelengths used above, the amount of the dyes in both fractions was determined

comparing the fluorescence intensity of the unknown samples with the standard samples (calibration curves previously constructed). Then, the Entrapment Efficiency was assessed using the Equation 3-4, presented below, where $m_{initial}$ is the mass of dye used to the production of nanoparticles and m_{losses} is the total amount of dye recovered from the polymer aggregates and dialysis.

$$Entrapment\ Efficiency\ (\%) = \frac{m_{\ initial} - m_{losses}}{m_{initial}} \times 100$$

Equation 3-4: Entrapment efficiency of compounds in the PLA nanoparticles.

Along with the previously quantification of total dye encapsulated in nanoparticles ($m_{encapsulated\ dye}$), it was also determined the amount of PLA that form particles ($m_{nanoparticles}$), using the method described in the section about "Yield of Nanoparticles". Thus, with the Equation 3-5, it was possible to obtain the loading efficiency, which corresponds to the amount of dye per milligram of nanoparticles.

For the entrapment efficiency and loading efficiency, the measurements were made at least three times and the results were expressed as mean value ± standard deviation.

$$Loading\ Efficiency\ (\%) = \frac{m_{encapsulated\ dye}}{m_{nanoparticles}} \times 100$$

Equation 3-5: Loading efficiency of the dyes in the PLA nanoparticles.

3.2.4.2. *In vitro* Release Profile and Dye Release Kinetics

In vitro release behavior of Nile Red and FITC from the PLA nanoparticles was studied with a two-phase system (hydrophilic/lipophilic) using water and isopropyl myristate (IPM); IPM was used due to its composition, which can mimic the lipophilic structure of the *stratum corneum* [45]. For that, 1 mL of aqueous suspension of

nanoparticles (containing either Nile Red or FITC) was added to the same volume of IPM. For particles containing NR, the system was constantly stirred (50 rpm) at 37 °C, and small aliquots (10 µL) of the lipophilic phase (receptor medium) were collected and replaced with the same volume of IPM at fixed time points (0, 1, 2, 4, 6, 8, 12 and 24h). The aliquots were restored with the lipophilic solvent and the fluorescence intensity was measured by UV-Spectrophotometry using 520 nm and 570 nm as excitation and emission wavelengths, respectively [33]. In the case of particles loaded with FITC, the release tests were also performed at 37 ˚C, with stirring rate of 50 rpm. At the same fixed time points used for Nile Red, the hydrophilic phase was collected and centrifuged at 3000 g for 15 min, to separate nanoparticles from the free dye. Then, an aliquot of the supernatant was withdrawn, restored with distillated water and the fluorescence was measured by UV-Spectrophotometry; excitation and emission wavelengths were 495 and 525 nm, respectively. Finally, the supernatant was discharged and the nanoparticles were ressuspendend with 1 mL of water; the particle suspension was added again to the lipophilic phase and incubated at the same conditions [80]. The concentration of the released dyes was determined comparing the fluorescence intensity of unknown samples to that of standard samples (calibration curves previously constructed), in order to establish the release rates of Nile Red and FITC from nanoparticles. The *in vitro* release study of the fluorochromes from nanoparticles was carried out in triplicate.

With the release rates of fluorochromes, it was possible to achieve the release behavior of the dyes from the PLA nanoparticles. Thus, the release data was fitting to the empirical relationship given by Ritger-Peppas equation (Equation 3-6) [20].

$$\frac{M_t}{M_\infty} = k \times t^n$$

Equation 3-6: Ritger-Peppas equation.

The *n* value on the equation is the diffusion exponent characteristic of the release mechanism and it is given by the relation between the fraction of drug

released at time t (M_t/M_∞); t is the release time and k is the kinetic constant. To determine the value of *n*, the Equation of Ritger-Peppas is transformed (Equation 3-7) and *n* is the slope value of the plot of log (% release) *versus* log t [20].

$$\log(\%\ \text{released}) = \log\left(\frac{M_T}{M_\infty}\right) = \log k + n \times \log t$$

Equation 3-7: Ritger-Peppas modified equation.

3.2.5. *In vitro* Follicular Penetration Studies

In vitro follicular penetration studies of topically applied PLA particles (obtained with agitation and ultrasound, containing hydrophilic or lipophilic dyes) were carried out using Franz diffusion cells (Figure 3-1). These diffusion cells consist of a donor compartment and a receptor compartment among which a membrane (biological or artificial) is mounted; an O-Ring is used to position the membrane. The two cell compartments are hold together with a clamp and the temperature in the receptor chamber is controlled by a circulating water bath. In this work, the receptor compartment was filled with 5 mL of phosphate buffered saline (PBS, pH 7.4), thermostatically maintained at 37 °C, that was continuously stirred at 600 rpm with a magnetic bar. Both compartments were sealed with aluminum foil to prevent evaporation of the solutions.

3.4.5.1. Preparation of the Skin

In this study, pig skin was used due to its resemblance with human skin regards to permeability [81]. Before experiments with skin, subcutaneous fat was carefully removed using forceps and a scalpel, the skin was cut into individuals sections of appropriate size and the surface was cleaned with PBS (pH 7.4). Finally, the skin was inspected macroscopically and microscopically (using light microscopy after staining

with haematoxilin and eosin) for tissue damage. Immediately after its preparation, the skin was used.

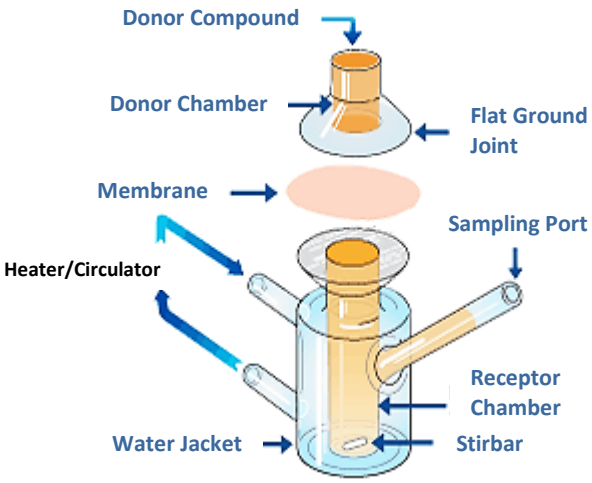

Figure 3-1: Sketch of a typical Franz Diffusion Cell (Online image, available at http://www.permegear.com/fc01.gif; accessed on October 11, 2012).

3.4.5.2. Application of Particles on Skin Explants

The skin was mounted in Franz Diffusion Cells with the *stratum corneum* facing the donor compartment and the dermis facing the receptor compartment. The tissue was allowed to acclimatize to the receptor phase for 15 min and then, particles suspensions (300 µL) were applied on the skin surface and incubated for 24h. In order to compare the ability of particles produced with different methodologies to penetrate inside the hair follicles, Nile Red-loaded nanoparticles obtained with agitation and sonication were used. FITC-loaded nanoparticles produced with agitation were also incubated with skin samples to determine if the nature of the entrapped compound has influence on the penetration profile of PLA-NPs produced in this study. After incubation with the particles, the skin samples were washed in first place with ethanolic solutions (100%, v/v; 75%, v/v; 50%, v/v) and then with PBS (pH 7.4) to remove NPs that had not penetrated into the skin; finally, the samples were wiped. As negative control, untreated skin was used.

3.4.5.3. Cryosections and Fluorescence Microscopy

The penetration of PLA-NPs into hair follicles was investigated on skin cryosections with fluorescence microscopy. After skin incubation with nanoparticles containing fluorescent dyes, the skin samples were embedded in cryocompound Neg-50 Frozen Section Medium (Thermo Scientific Inc., Bremen, Germany), frozen in liquid nitrogen and finally they were cut vertically with fresh blades into 20 µm thickness cryosections using a cryostat. Hair follicles from skin areas treated with particle-containing formulations were obtained; to avoid counting the same hair follicle twice, once obtained a central section of a hair follicle, the next 2-5 sections were excluded. The cryosections were mounted on glass slides and visualized by bright field and fluorescence microscopy in a microscope equipped with a filter for FITC and Nile Red. By superposition of the images, the maximal depth reached by nanoparticles was classified accordingly to Figure 3-2.

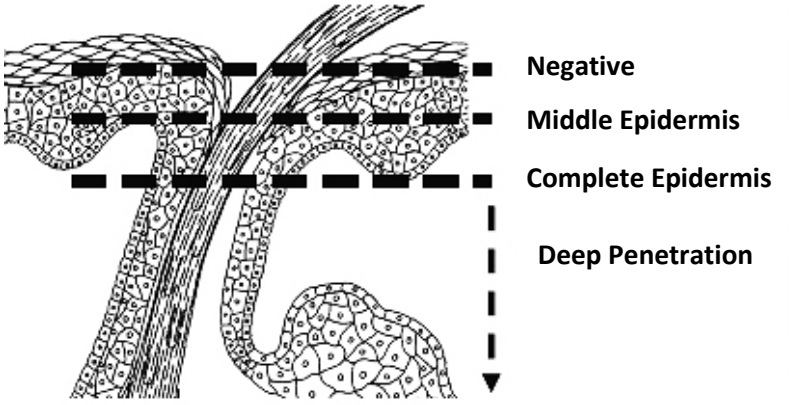

Figure 3-2: Depth of penetration of PLA nanoparticles into the hair follicles, after topical application (Adapted from Rancan F. *et al.*, 2009 [45]).

4. RESULTS AND DISCUSSION

4.1. Preparation of PLA Nanoparticles

Firstly, nanoprecipitation method was used to produce PLA nanoparticles. Since these particles are intended for hair follicle targeting, their size should be as small as possible, assuring a deeply penetration into the follicles, but not less than 100 nm to avoid their translocation into the viable epidermis of intact skin [45].

The produced particles should be stable and ζ-potential (measure of the surface charge of the particles) was used to predict their stability; as the ζ-potential increases, the repulsive interactions will be larger (preventing aggregation), increasing the stability of the nanoparticles dispersion. A colloidal dispersion of charged particles only stabilized by electrostatic repulsion is considered stable when Zeta-Potential have a minimum value of ± 30 mV [69].

4.1.1. Comparison of Preparation Techniques

In order to obtain smaller particles than nanoprecipitation usually provides, some alterations to the standard method were introduced, accordingly to three different techniques: agitation, sonication and homogenization.

Regarding to sonication, it is known that the depth of probe tip from the base of the vessel, the power input and the duration of treatment can influence the ultrasound conditions imposed in the solution, affecting the size range and ζ-potential of the particles obtained. Thus, based on the results obtained by Silva *et al.* (2010), the nanoparticles were produced at 19 mm of depth (anti-nodal point; λ/4), where the amplitude of the wave is a maximum, and 40% of power input. Using these conditions, the authors reported that highest values of energy input are achieved, the cavitation phenomenon is more pronounced promoting a higher hydroxyl radicals ($^{\bullet}OH$) formation, greater shear forces are exerted and a higher mixing of the solution is obtained, allowing the formation of particles with the lowest sizes and the highest homogeneity [82]. Concerning to the duration of the treatment, using the mentioned conditions, two times (15 and 18 min) were tested in order to understand its effect on

the properties of PLA nanoparticles. In Figure 4-1, it can be seen that particles obtained with 18 min of sonication were substantially smaller and more homogeneous than those obtained with 15 min of treatment. It is proposed that, for 18 min of sonication, the amount of energy supplied to the system was greater, increasing the shear stress, which caused a more efficient particle breakdown resulting in a decrease of the mean diameter and PDI of particles [39]. About the measurements of ζ-potential, no significant differences were found amongst the tested times (data not shown), showing that the time of sonication did not change the stability of particles produced.

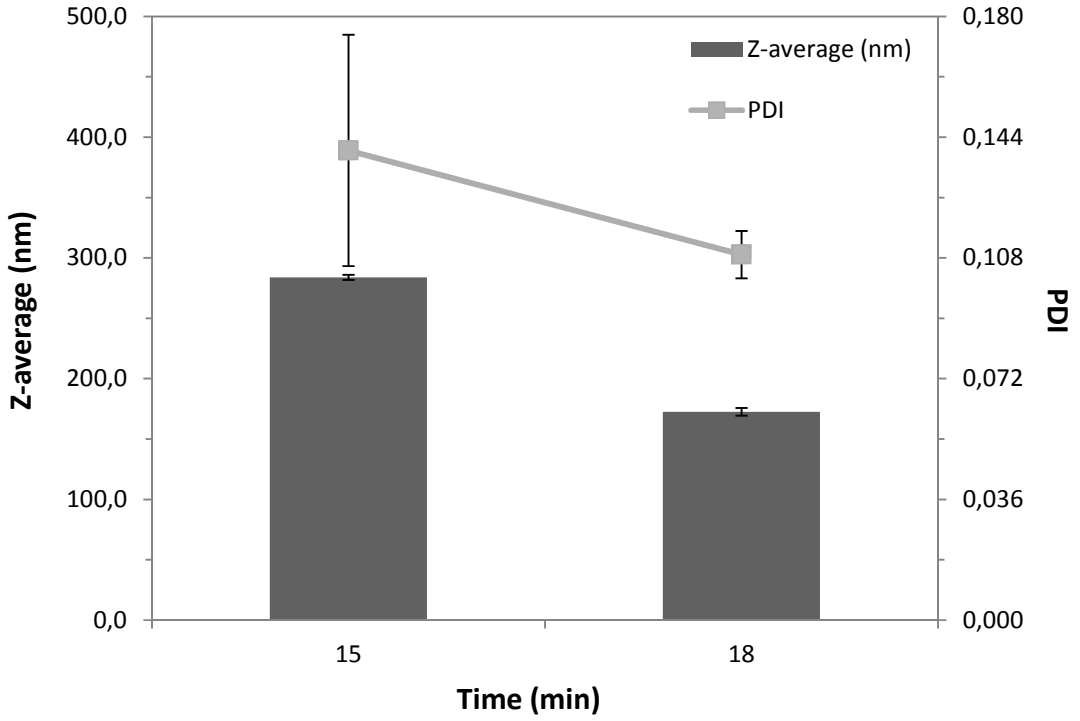

Figure 4-1: Mean size and size distribution (PDI) of PLA nanoparticles, obtained after a sonication treatment of 15 and 18 minutes.

After the initial optimization of the conditions for the production of PLA nanocarriers with ultrasound, nanoparticles were prepared employing the three techniques. So that the results obtained with the different techniques were as comparable as possible, the same time (18 min) was used for the production of

particles with sonication and homogenization. The size, PDI and ζ-potential of particles obtained with the different techniques are shown in Table 4-1.

Table 4-1: Effect of the employed techniques on the properties of PLA nanoparticles, obtained by nanoprecipitation.

	Z-average (nm) ± SD	Polydispersity Index ± SD	Zeta-Potential (mV) ± SD
Agitation	161.4 ± 0.4	0.047 ± 0.003	-20.0 ± 0.1
Sonication	172.6 ± 2.1	0.109 ± 0.007	-19.6 ± 0.2
Homogenization	640.2 ± 71.3	0.146 ± 0.015	-20.0 ± 1.4

As expected, surface charge of nanoparticles was negative. It is known that PLA chains have carboxyl groups at their extremity and, when they aggregate to form nanoparticles, these groups tends to be located in the aqueous environment, creating a negative surface charge [83]. Attending to the values of ζ-potential, as they were higher than -30 mV, nanoparticle suspensions seemed to have only moderated stability. However, it has to be notice that a non-ionic surfactant (Pluronic F68) was used and therefore, the effect of steric stabilization (surfactants or other molecules at the particle surface) must be taken into account [84]. Once the adsorbed layer of Pluronic F68 can partially masks the carboxyl groups at the surface of nanoparticles (due to the shift in the shear plane of the particles), it will leads to a decrease in the surface charge (absolute value) of nanoparticles [83]. Thus, the ζ-potential obtained is sufficient to keep the system stable under the steric stabilization offered by Pluronic F68 chains. Finally, as the differences on ζ-potential were neglectable, it could be assumed that all the techniques produced particles with similar stability.

While the duration of treatment was the same, particles produced with homogenization had larger mean diameter than those produced by sonication; the

population of particles obtained with the homogenizer was also more heterogeneous than the population obtained with the sonicator (Table 4-1). Since the most direct influence on the shear stress is exercised by the energy density (external energy applied per unit total volume), and the magnitude of shear stress is inversely correlated to the size of particles, it is possible that energy provided to solution by sonication was higher, explaining the improved properties of particles obtained with sonochemical treatment [39]. Moreover, the production of free radicals in solution is much more pronounced with ultrasound than with the homogenizer. This may also have been responsible for the results obtained as the interference of these free radicals with the nanoparticles is more extensive in sonication, helping in the reduction of their size [82, 85].

Despite the particles produced with ultrasound were smaller than those produced with homogenization, NPs produced with agitation were even smaller and more homogeneous than particles produced by sonication. The dropwise addition used in this technique can be the major responsible for the particle size obtained. It is known that the formation of NPs via nanoprecipitation is caused by the nucleation of small aggregates of macromolecules followed by the aggregation of these nuclei [86]. As dropwise addition can induce a better spread of the organic phase into the aqueous phase, it is possible that aggregates formed were smaller than those obtained with sonication and homogenization in which the PLA solution was added to the outer phase, all at once. Consequently, smaller aggregates of macromolecules conducted to the formation of smaller particles. Another explanation for the results obtained can be attributed to the rate of diffusion of the solvent into the aqueous phase; as the ratio aqueous phase to organic phase increases, there is a faster diffusion of the solvent into the outer phase and smaller particles are produced [39, 87]. Thus, in agitation, for every drop added to aqueous solution, the ratio aqueous to organic phase was much more higher than the ratio obtained for the addition of the organic solution all at once (sonication and homogenization), leading to a faster diffusion of the solvent from each droplet and consequently to the formation of smaller particles. The further overnight agitation provided enough mechanical force to the solution to decrease even more the size of particles, also promoting a greater homogeneity.

4.1.2. Influence of the Solvent Phase

According to Fessi *et al.* (1986), the addition of a portion of a non-solvent to the solvent phase can be advantageous for the production of smaller nanoparticles by nanoprecipitation [66]. Thus, in this experiment, it was tested the influence of two binary mixtures - Acetone/Water (90/10, v/v) and Acetone/Ethanol (45/55, v/v) - on the properties of PLA nanoparticles, prepared with agitation and sonication. As it can be seen in Table 4-2, the size of particles was markedly affected by the nature of the solvent, with both techniques showing an increase on the mean diameter of nanoparticles in the following order: Acetone/Ethanol < Acetone < Acetone/Water.

Table 4-2: Effect of the solvent phase on the properties of PLA nanoparticles, prepared with agitation and sonication.

	Solvent Phase	Z-average (nm) ± SD	Polydispersity Index ± SD	Zeta-Potential (mV) ± SD
Agitation	Acetone	161.4 ± 0.4	0.047 ± 0.003	-20.0 ± 0.1
	Acetone/Water	170.2 ± 4.3	0.081 ± 0.011	-20.9 ± 2.0
	Acetone/Ethanol	146.1 ± 1.6	0.078 ± 0.007	-21.5 ± 1.3
Sonication	Acetone	172.6 ± 2.1	0.109 ± 0.007	-19.6 ± 0.2
	Acetone/Water	196.4 ± 14.0	0.126 ± 0.019	-22.1 ± 0.3
	Acetone/Ethanol	146. 5 ± 8.1	0.123 ± 0.015	-22.9 ± 3.4

To some extent, the results obtained can be explained attending to the interactions organic phase-aqueous phase in the formulation. When the polymer-containing solution is dispensed into the aqueous phase, the higher the affinity of the

solvent to water, the faster its diffusion and particles with smaller sizes are formed [88-90]. The affinity of a solvent to water is given by its polarity which in turn is related to its dielectric constant (higher dielectric constant corresponds to higher polarity). The dielectric constant of acetone, water and ethanol are mentioned on the literature as 21, 80 and 30, respectively. On the other hand, the dielectric constants of the mixtures used in this work were determined theoretically from the Equation 4-1.

$$E = \frac{\%Acetone\ E(A) + \ \%B\ E(B)}{100}$$

E = Dielectric constant of the mixture

E(A) = Dielectric constant of Acetone

E(B) = Dielectric constant of Water or Ethanol

%Acetone = Content of Acetone in mixture (%)

%B = Content of Water or Ethanol in mixture (%)

Equation 4-1: Theoretical determination of dielectric constant of the mixtures of solvents.

The dielectric constants for the mixtures Acetone/Water (90/10, v/v) and Acetone/Ethanol (45/55, v/v) are 26.9 and 25.95, respectively [90]. Attending to the values obtained, the dielectric constants can explain why nanoparticles obtained with a mixture of Acetone/Ethanol (45/55, v/v) are smaller than those obtained with Acetone. On the contrary, as the mixture of Acetone/Water (90/10, v/v) has the highest dielectric constant amongst the three tested solvent phases, the particles produced should have the smallest sizes but the results obtained showed the opposite. Thus, to completely understand these results, the affinity of PLA to the solvent (polymer-solvent interactions) must also be taken into account.

As the affinity of PLA to the solvent increases, the polymer can be better dispersed, leading to chains more detangled from one another and an extensively

solvation occur. Contrarily, when the affinity of the polymer to the solvent decreases, the chains become more shrunken, forming a solution with increased intrinsic viscosity that avoids an efficient diffusion of the organic phase; since there is no separation of the polymer chains, they have tendency to overlap. Due to the limited solvation, when the water penetrates in regions between the chains, the isolation of larger cluster occurs and particles with larger sizes are obtained [87, 91]. For sonication, an increase of the viscous forces in solution will also opposes to the shear stress produced by ultrasound, decreasing the net shear stress available for particle breakdown, producing particles with increased size [39]. Since acetone is a solvent for PLA, the polymer has a great affinity to it. Concerning to water and ethanol (both non solvent), the affinity was determined experimentally; water showed less affinity for PLA than ethanol because a lower percentage (10%) of water was necessary the reach the cloud point (maximum fraction of non-solvent in the mixture with acetone to continue to be complete dissolution of the polymer) when compared to ethanol (55%). Thus, attending to the interactions polymer-solvent, it is now more acceptable that the mixture Acetone/Water (90/10, v/v) had produced the particles with the larger sizes for both techniques because, despite its diffusion rate was the faster, it was not enough to counteract the negative effects of the increased viscosity of the system. On the other hand, it is hypothesized that the decreased affinity of PLA to the mixture Acetone/Ethanol (45/55, v/v) when compared to acetone was not enough to attenuate the effect of its faster diffusion into the aqueous phase whereby, PLA-NPs produced with this mixture had smaller sizes.

About the size distribution of nanoparticles, for both techniques, the homogeneity (PDI) was slightly (not significant) increased in the following order: Acetone < Acetone/Ethanol < Acetone/Water (Table 4-2). As it can be seen, there was a correlation between the affinity of the solvent to the polymer and the polydispersity index obtained, confirming once again that this parameter can be an important factor related to the formation of nanoparticles, using the nanoprecipitation method.

Attending to ζ-potential (Table 4-2), for both techniques, the particles obtained with the different solvents were very similar regarding to the stability.

4.1.3. Effect of the Surfactant Concentration

Nanoparticles produced by nanoprecipitation can generate colloidal stability even without the presence of a surfactant. However, its utilization can be advantageous to obtain particles with smaller sizes and PDI, as it will be adsorbed on the surface of the nanoparticles, lowering their surface energy and hence reducing coalescence and agglomeration promoted by the gradual increase in droplet viscosity as the organic phase diffuses into the aqueous phase [66, 78, 83]. Consequently, in the previous steps of this work, a 0.6 % (w/w) of Pluronic F68 was employed in the formulations; even if this amount of stabilizer had been proved enough to obtain adequate nanocarriers for follicular targeting, the concentration of surfactant in the formulation was varied to analyze its effect on the properties of the particles and the results are shown in Figure 4-2.

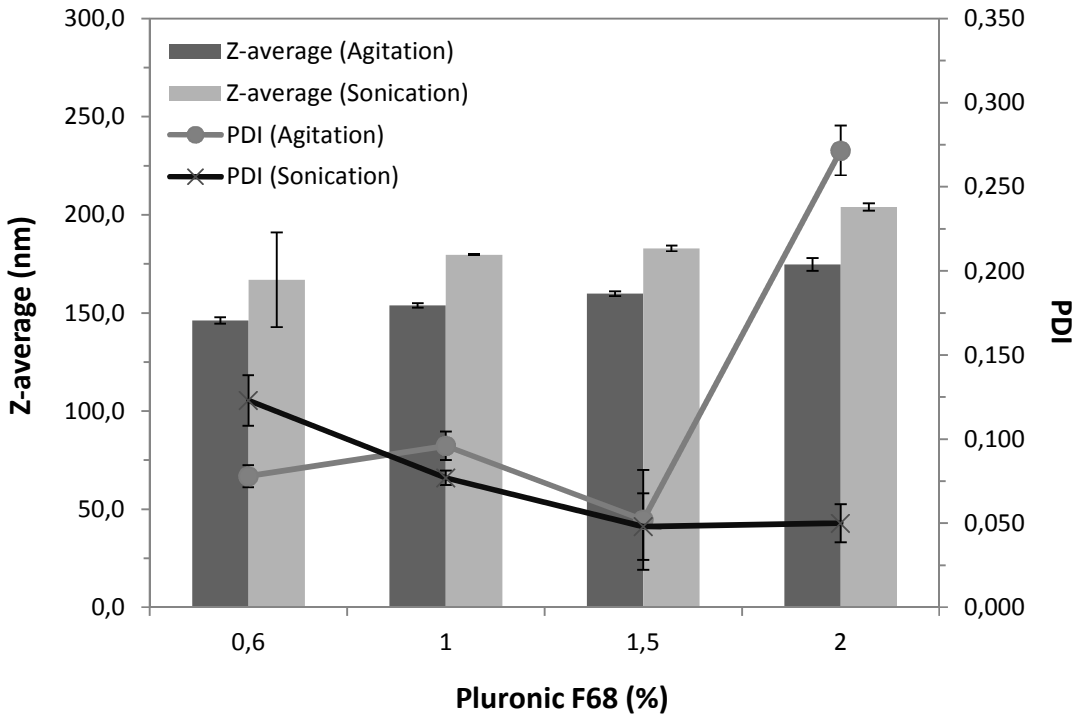

Figure 4-2: Effect of Pluronic F68 on the size and PDI of nanoparticles produced by nanoprecipitation, using agitation and sonication.

The results obtained in this study show that an increase in surfactant concentration increased the size of nanoparticles; similar results have also been reported in the literature [33, 90, 92, 93]. For polymeric surfactants, such as Pluronic F68, an increase in their concentration is responsible for an enhancement of the viscosity of the aqueous phase which can decreases the wavy movement and collision of the particles, avoiding its aggregation and promoting the formation of particles with smaller sizes [84]. However, as the viscosity of the aqueous phase increases, the diffusion of the organic phase into the aqueous phase can be hindered and a reduction in the net shear stress available for particle breakdown can occur, which promotes the formation of larger droplets and consequently leads to an increase on the mean size of particles (as observed in this work) [39, 90, 94].

Regarding to the polydispersity, there was a reduction on the PDI until 1.5% (w/w) of Pluronic F68. It is hypothesized that as more surfactant molecules were added to the solution, more stabilizer molecules overlaid the surface of particles, reducing their surface tension and improving protection from coalescence promoting a better homogeneity [78]. Above 1.5% of Pluronic F68, for sonication, the polydispersity remained practically the same probably because the saturation of surfactant that is packing at the surface of the particles was achieved and the stabilizer could no longer provide improved homogeneity [90, 92]. On the other hand, for agitation, a 2% (w/w) of Pluronic F68 increased the polydispersity of the solution possible due to the predominance of the effect of the viscosity over the stabilizer effect of the surfactant. The viscosity of the aqueous phase hindered an effective dispersion of the organic solution and since the mechanical stirring provided by agitation was not enough to counteract the effect of high viscosity, the organic phase was not well dispersed and the particles formed had very different sizes (particle population became more heterogeneous) [39, 84, 90, 94].

Attending to the stability, when agitation was used, ζ-potential changed scarcely with the increasing of Pluronic (0.6% (w/w): -21.1 ± 0.7 mV; 1% (w/w): -23.4 ± 0.3 mV; 1.5% (w/w): -18.6 ± 0.3 mV; 2% (w/w): -21.0 ± 0.6 mV). On the other hand, with ultrasound, there was a marked decrease on the absolute value of ζ-potential as the concentration of surfactant increased (0.6% (w/w): -22.7 ± 2.4 mV; 1% (w/w): -20.8

± 0.1 mV; 1.5% (w/w): -19.7 ± 0.2 mV; 2%(w/w): -15.9 ± 0.5 mV); nevertheless, this tendency must not be assumed as a decreasing in the stability of the particles. It is possible that ultrasound can promote a better adsorption of surfactant on the surface of particles than agitation and, as more surfactant molecules were adsorbed to the surface of particles, an increased screening of the carboxyl groups of PLA (responsible for the negative charge of nanoparticles) occurred, promoting a decrease in the particle charge.

4.2. Yield of Nanoparticles

The yield of nanoparticles is a decisive factor to evaluate the efficiency of a preparation method, especially on large industrial scale [78]. Thus, in this part of the work, the yield of nanoparticles was firstly determined for formulations prepared with a mixture Acetone/Ethanol (45/55, v/v). Then, once ethanol can influence the efficiency of nanoparticles formation (as reported by Jiang *et al.*, 2003), the effect of different volume fractions of this solvent in the organic phase were tested in order to clarify its effects on the yield of PLA nanoparticles [78]. In Figure 4-3, for agitation and sonication, the yields obtained are plotted against the volume fraction of ethanol in the binary mixture. For all the tested fractions, the measurement of nanoparticles yield, made on at least three different batches produced under identical conditions, fell within a range of 10%, indicating a good reproducibility of the results.

Since the production of large polymeric aggregates, either dispersed in the aqueous phase or adhered to the recipients, plays a key role on the yield of nanoparticles, they will be used to explain the results obtained; as the amount of aggregates that are not nanoparticles increases, the yield of nanoparticles decrease [68]. Attending to the technique, in agitation, the dropwise addition combined with continuous stirring promotes an efficient spread and a fast diffusion of the organic phase into the aqueous phase, which led to the precipitation of PLA mostly in the form of small nanoparticles that remained in suspension [18]. As this technique fails to form large aggregates, this is probably the reason why a low percentage of polymer stuck to

the recipients was recovered. In contrast, in sonication treatment, the PLA solution was added to the aqueous phase all at once, without mixing. When the two phases became in contact, since the molecules of PLA in the aqueous phase are not as well dispersed as in agitation and the diffusion is slower, it is hypothesized that more polymeric molecules can agglomerate to form large aggregates that due to its dimensions settle to the bottom of the containers; the results obtained confirmed this assumption. Relating to the aggregates dispersed in solution, as previously reported, agitation usually produce a population of nanoparticles more homogeneous than sonication; thence, for sonication, it is most likely to find a larger amount of nanoparticles that deviates from the average size and are above 1.2 μm. Consequently, this can explain why the percentage of polymeric agglomerates recovered after filtration was higher for the nanoparticles suspensions produced by ultrasound. In conclusion, as sonication produced higher percentage of large aggregates of PLA, the percentage of nanoparticles effectively formed was lower than those obtained for agitation, regardless of the fraction of ethanol.

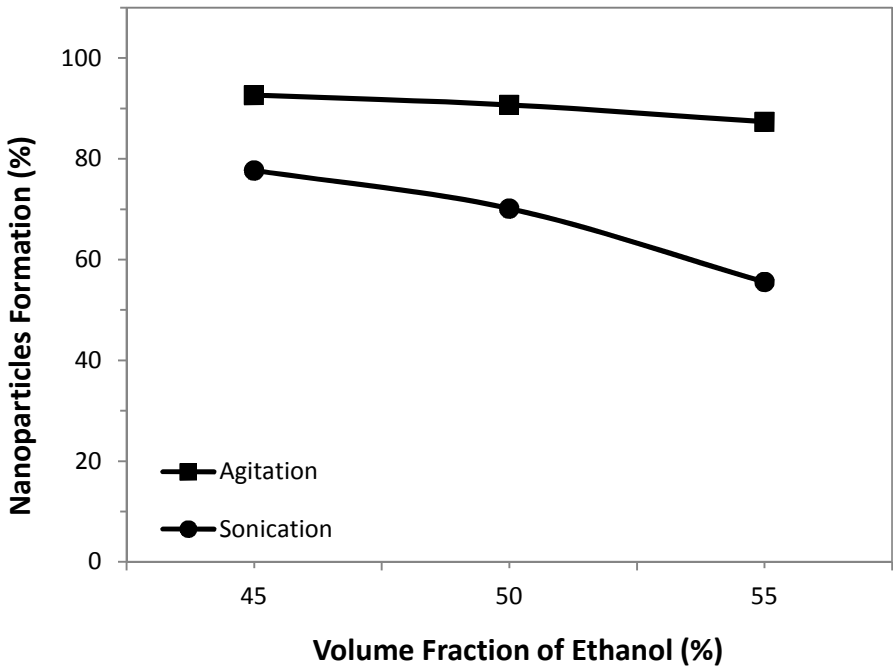

Figure 4-3: Effect of the volume fraction of ethanol on the yield of nanoparticles, prepared by nanoprecipitation.

Despite the differences between agitation and sonication, the effect of ethanol on the formation of nanoparticles was similar for both techniques: as the fraction of ethanol increased, the yield of nanoparticles decreased (Figure 4-3). It is known that an increase of the ethanol fraction increases the polarity of the binary organic solvent (Equation 4-1), leading to a faster diffusion of the solvent phase into the aqueous phase and consequent formation of smaller aggregates and formulations with higher yields of nanoparticles. However, is also mentioned on the literature that, as the diffusion process occurs faster, more polymer can immediately precipitates and deposit before agglomeration into particles occurs [39, 88-90]. This is one of the explanations for the increasing percentages of PLA agglomerates that were recovered from the containers, as the volume fractions of ethanol increased. Secondly, as the fraction of ethanol increases, the affinity of the polymer to the mixture decreases and there is an increasing on the viscosity of the solvent. Further, an increasing on viscosity of the organic phase will be responsible for the formation of higher amounts of larger agglomerates that will increase the amount of polymer recovered from the containing material or by filtration [87, 91].

In the first part of this work, it was proved that the polarity and viscosity of the organic phase can influence the properties of the nanoparticles. Thus, once different fractions of ethanol can promotes changes on these parameters of the organic phase, the size and PDI of nanoparticles, prepared with the tested fractions, were monitored - Figure 4-4. For sonication, when the fraction of ethanol increased, the size and PDI decreased. Moreover, although the differences between 55% and 50% were not significant, when the fraction of ethanol decreased to 45%, it was verified a marked increase on the size of nanoparticles. This results are consistent with the expected because, an increasing in the fraction of ethanol leads to a faster diffusion of the organic phase, which in turn promotes the formation of smaller and more homogeneous nanoparticles [88, 89, 115]. Despite the viscosity of the organic increases for higher fractions of ethanol (which can increase the size of particle), the viscous forces were probably not sufficient to counteract the effect of the ratio of diffusion of the organic phase [87, 91]. Regarding to agitation, increasing the volume fraction of ethanol from 50% to 55% also led to a slightly decrease on the mean size of

the particles. However, with a 45% of ethanol on the binary mixture, instead of the increasing on the particles size due to the slower diffusion of the solvent, it was showed a considerable decrease on the mean diameter. This probably happened because of the increased interactions polymer-organic phase that supplanted the effect of the interactions organic phase-aqueous phase.

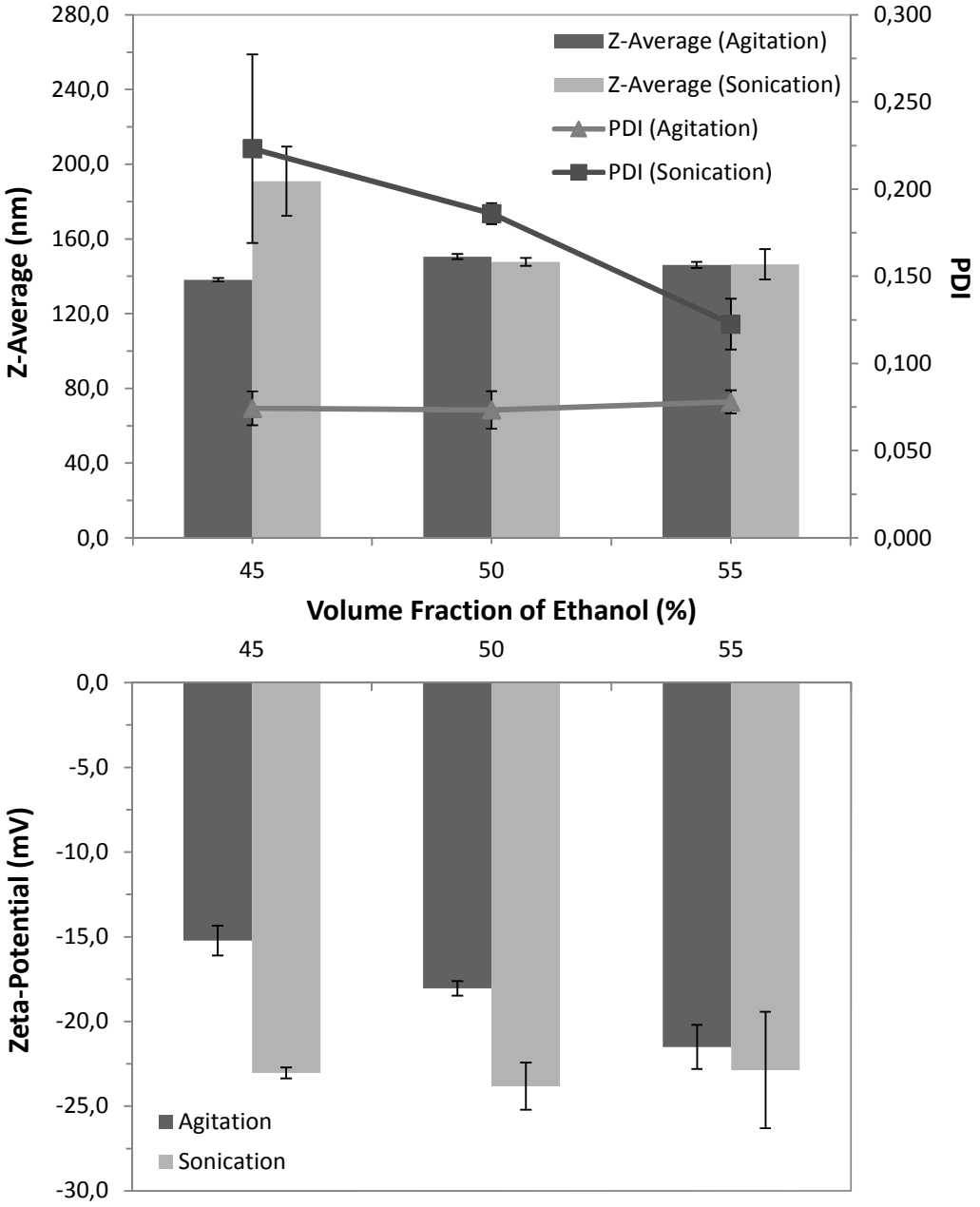

Figure 4-4: Effect of volume fraction of ethanol on the properties of PLA nanoparticles, prepared with agitation and sonication.

Finally, changes on ζ-potential of nanoparticles, as a result of the fraction of ethanol, were also investigated (Figure 4-4). As it can be seen, for sonication, the stability of nanoparticles produced with increasing volume fractions of ethanol remained practically unchanged since the values of ζ-potential were very similar. On the other hand, there was a decreasing (absolute value) on surface charge of particles produced by agitation, as the volume fraction of ethanol decreased. For particles produced with 45% of ethanol on the binary mixture, the value of ζ-potential was especially high (-15.2 ± 0.9 mV), which can be problematic as it can leads to aggregation of nanoparticles during the storage.

4.3. Morphology of Nanoparticles

The characterization of particles surface is important in the context of controlled release of active ingredients. Therefore, a NOVA Nano SEM 200 FEI was used to visualize the nanoparticles previously prepared, using Acetone/Ethanol (50/50, v/v) and a Pluronic F68 concentration of 0.6 % (w/w). Figure 4-5 shows the STEM photographs obtained for PLA nanoparticles produced by nanoprecipitation, using agitation and sonication. As the total amount of polymer was distributed homogeneously through the solution during nanoprecipitation, the preferred shape of the particles was spherical [85]. This morphology would offer the highest potential for controlled release and protection of incorporated drugs as they provide minimum contact with the aqueous environment as well as the longest diffusion pathways [84].

Even slightly agglomerated due to the high concentration on the sample, nanoparticles seemed to have smooth surfaces and they showed clearly homogeneity. However, as expected, the size distribution of NPs produced by agitation was narrow when compared to those obtained by sonication.

Finally, regarding to the mean size of nanoparticles, the results obtained with STEM are also in good agreement with the measurements made by PCS.

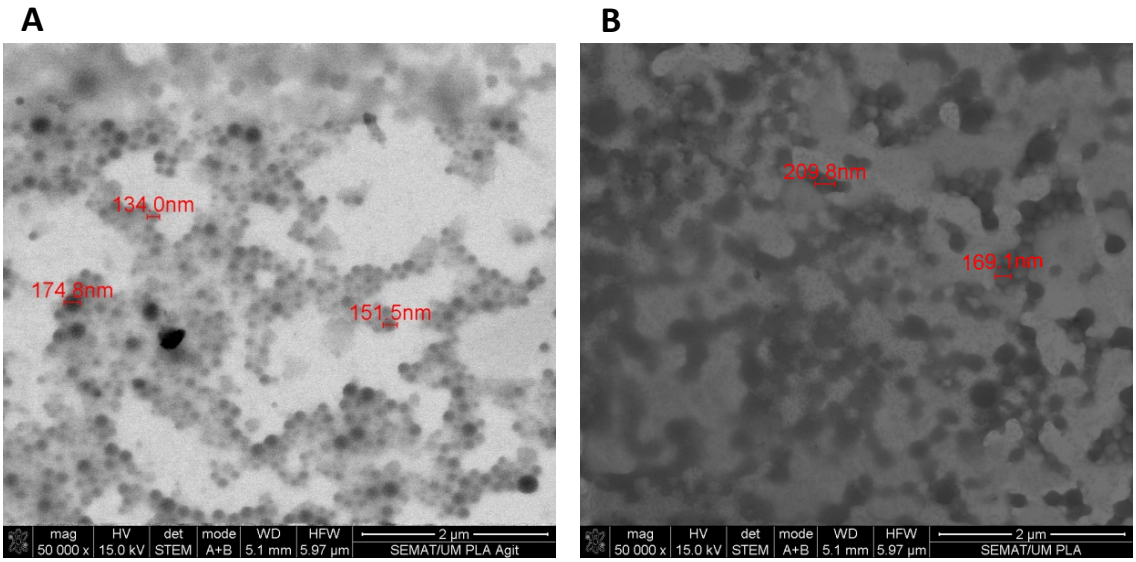

Figure 4-5: **S-TEM photographs (x50000 magnification) of PLA nanoparticles obtained with A) agitation and B) sonication, using a binary mixture of Acetone/Ethanol (50/50, v/v) and Pluronic F68 concentration of 0.6% (w/w).**

4.4. Encapsulation of Model Compounds

In drug delivery, apart from the yield and the properties of the carriers, the success of a formulation is mostly related to the capacity of particles to entrap bioactive agents. Thereby, Nile Red or FITC (lipophilic and hydrophilic model compounds, respectively) along with PLA were dissolved in a mixture of Acetone/Ethanol (50/50, v/v), in order to produce loaded nanoparticles.

Figure 4-6 shows the size, PDI and ζ-potential of nanoparticles obtained with agitation and sonication. As demonstrated by the graph, after the incorporation of dyes, the changes in the mean diameter and PDI of nanoparticles produced with both techniques were meaningless. Regarding to the ζ-potential results, it can be notice that the presence of the dyes did not change the stability of nanoparticles since the surface charge was not affected significantly.

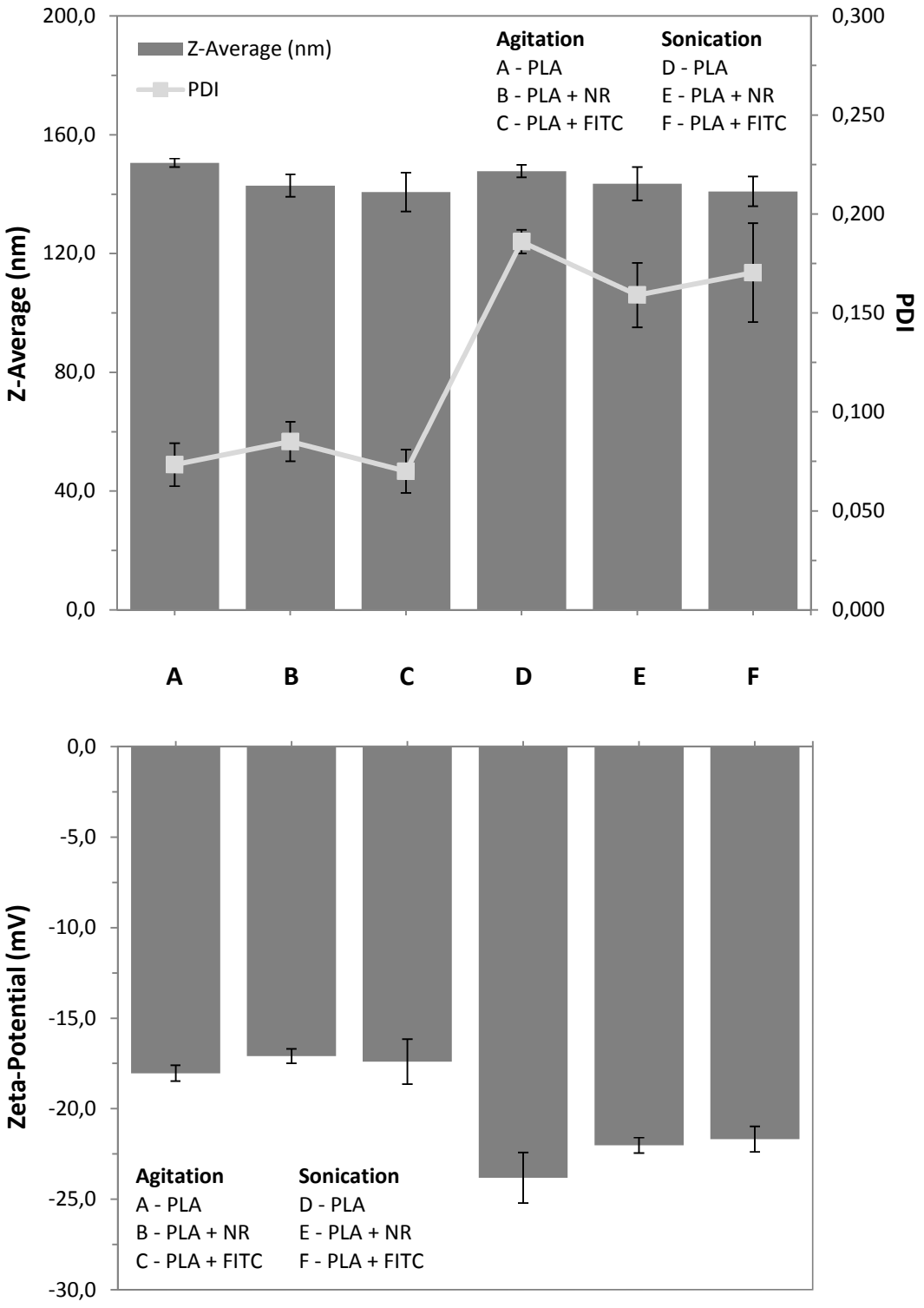

Figure 4-6: **Z-Average (nm), PDI and Zeta-Potential (mV) of PLA nanoparticles, prepared with agitation and sonication, after the entrapment of Nile Red and FITC.**

4.4.1. Entrapment Efficiency

The entrapment efficiency (ratio of quantity entrapped/adsorbed compound in relation to the total amount of compound used) is an important factor for drug delivery systems, once the release rate is usually dependent on the concentration of the bioactive agent inside nanoparticles [95]. Thus, after the production of dye loaded nanoparticles, the portion of fluorochromes not incorporated was quantified spectrophotometrically, in order to achieve the entrapment efficiency of lipophilic and hydrophilic molecules into PLA nanoparticles. For agitation and sonication, the incorporation of model compounds proved to be efficient and the results obtained are shown in Figure 4-7.

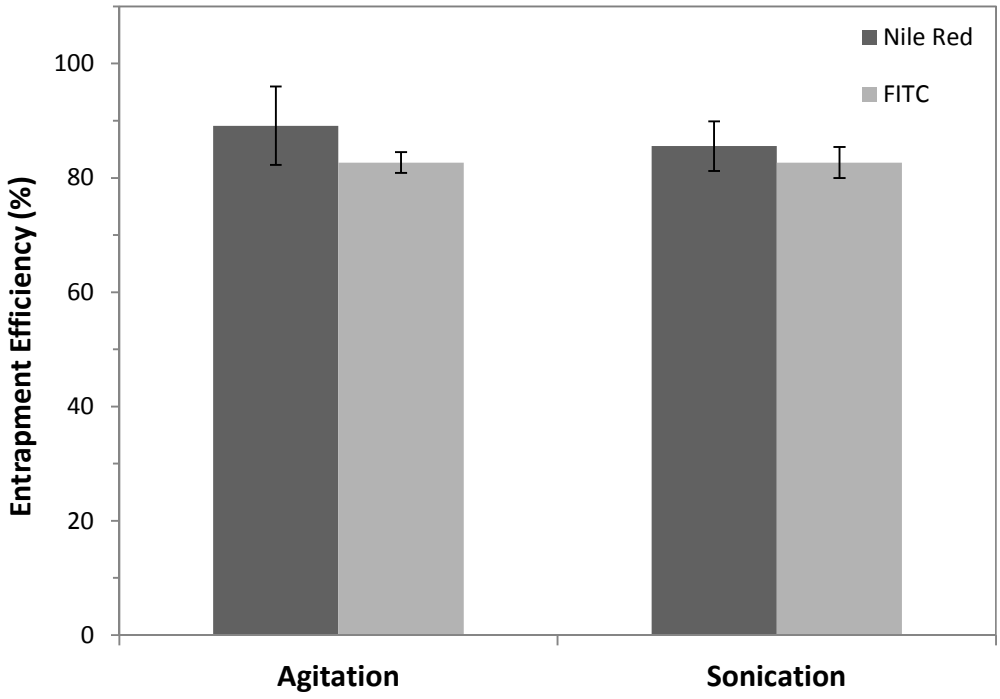

Figure 4-7: Entrapment efficiency of Nile Red and FITC into PLA nanoparticles, produced with agitation and sonication.

Figure 4-7 also shows that encapsulation of Nile Red was slightly higher for particles produced with agitation. This difference on the results can be explained

according to the diffusion rate of the organic phase into the aqueous phase. In nanoprecipitation, it is known that the entrapment of compounds occurs as a result of polymer precipitation, followed by solidification that leads to the formation of nanoparticles [39]. In turn, the solidification of nanoparticles is related to the ratio of diffusion of the organic phase. When the organic phase has low affinity to the continuous phase, the diffusion is slow, hindering the solidification of nanoparticles. Then, the complete portioning of the encapsulated compounds into the aqueous phase is facilitated as the compounds have more time to diffuse into the aqueous phase along with the organic phase [91]. Thus, as it was previously reported, when compared to sonication the diffusion of the solvents is faster in agitation because of dropwise addition; as the time to the compounds diffuse is lower, the amount of encapsulated compound increases.

Regarding to the incorporation of FITC, the results obtained are surprising taking into account that usually, nanoprecipitation is ineffective to encapsulate hydrophilic compounds; due to its water-soluble nature, they rapid partioning from the organic phase into the aqueous phase, leading to considerable losses in the continuous phase [91]. However, probably due to the properties of the binary mixture, it is possible that its diffusion rate and consequently solidification of the nanoparticles was so fast that leakage of large amounts of FITC was avoided. Other properties of the formulation, as viscosity of the organic phase and interactions polymer-drug, can also helped to increase the diffusional resistance of FITC, since they were previously involved on the achievement of high encapsulation efficiency of some molecules [39].

In addition to the entrapment efficiency, the loading efficiency was also determined for both dyes. The drug loading provides a measure of the amount of entrapped compound compared to the effective mass of nanoparticles [18]. Table 4-3 shows the differences in dye loading percentages. Since the formulation had similar entrapment efficiencies but the yield of nanoparticles was higher for agitation, it is not surprising that sonication had the highest loading efficiencies.

Table 4-3: Loading efficiency of Nile Red and FITC into nanoparticles produced by nanoprecipitation, using agitation and sonication.

	Nile Red (%) ± SD	FITC (%) ± SD
Agitation	0.0488 ± 0.0019	0.0508 ± 0.0004
Sonication	0.0608 ± 0.0058	0.0617 ± 0.0035

4.4.2. *In vitro* Release Profile

Nanoparticles prepared in this study aimed to be used for drug delivery and, one important feature of these carriers is their release profile. Thus, the *in vitro* release of Nile Red and FITC from PLA nanoparticles was studied in a biphasic system, consisting in an organic lipophilic solvent (IPM) and an aqueous solution [45]. The release studies were performed with this system because, firstly, PLA particles are stable in aqueous suspensions and no release of the dyes is observed for particles kept in water for long periods of time (the release is a slow process which occurs only upon polymer hydrolysis and particle erosion). Furthermore, as these particles are intended for topical application, IPM can mimics the lipophilic environment of the skin (chemical structure of IPM resemble that of sebum components) and consequently, the IPM/Water system can simulate the interface between the NPs aqueous suspension and the sebum on the skin surface and in the hair follicle ducts [45]. For PLA nanoparticles produced by the different techniques, the release profile of lipophilic and hydrophilic models are shown in Figure 4-8. In all kinetic profiles, the *in vitro* release exhibited a typical biphasic release phenomenon with an initial burst release in the first four hours followed by a constant slow release over the remaining time. Normally, the burst release is attributed to the fraction of the drug which is adsorbed or weakly bound to the large surface area of NPs or entrapped in the matrix near to

the surface of particles; slow and constant rate may be due to the diffusion of compounds, as well as to the erosion of the polymeric matrix [62, 96].

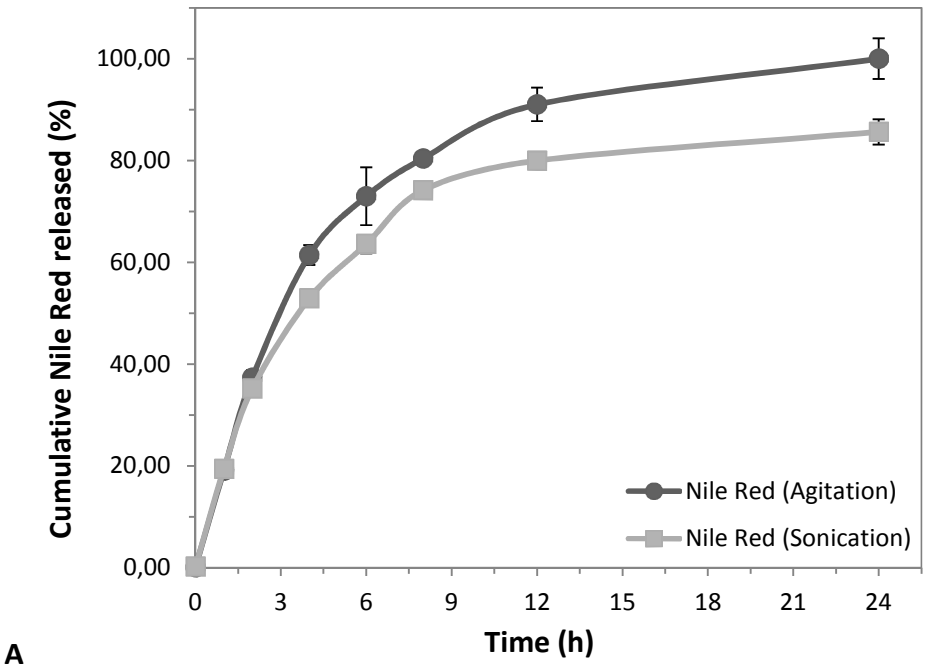

A

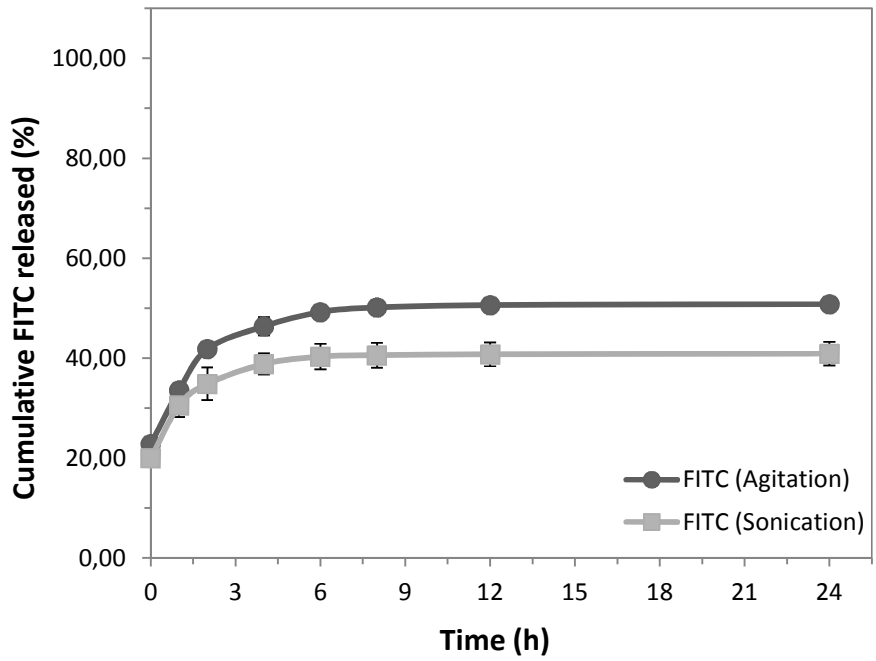

B

Figure 4-8: ***In vitro*** **release profile of A) Nile Red and B) FITC from PLA-NPs, produced by nanoprecipitation with agitation and sonication.**

Regardless of their nature, the release of dyes was faster for PLA nanoparticles produced with agitation. This can be due to the differences in drug loading obtained for particles produced with the different techniques; for both dyes, higher drug loading were achieved for particles produced by sonication (Table 4-3). Several reports have showing that a compound can be slowly released in higher drug contents because higher concentration leads to crystallization of compounds inside the nanoparticles and the compound should dissolve first from the crystal and then diffuses from the matrix (dissolution model), which reduces the compound release rate [97, 98].

Attending to the differences in the release of different dyes, when particles were placed in contact with IPM (t=0h), higher concentrations of FITC than Nile Red were measured on the outside of nanoparticles. During the formation of nanoparticles, FITC have a large tendency to rapidly partioning into the aqueous phase due to its hydrophilic nature; usually, this leads to an inefficient entrapment of hydrophilic compounds in the nanoparticles. However, in this study, it is hypothesized that binary mixture used to dissolve the polymer and the dye promoted a solidification of the particles so fast that losses of large amounts of the dye into the aqueous phase were avoided. Thus, since the solidification of the particles is made from the periphery, it is possible that high amounts of FITC that were trying to diffuse into the aqueous phase were entrapped in the matrix of the nanoparticles near to the surface or they were just adsorbed to the particle surface [69, 99]. Thus, when particles were added to IPM, due to the destabilization of the particles, an immediately released of FITC that were poorly entrapped in the particles occurred. As larger amounts of FITC than Nile Red were poorly entrapped, this explained why the differences in the released compounds at the first time point (0h). However, after the first time point, the lipophilic compound showed a fast release from the nanoparticles. As it can be seen in Figure 4-9, after 24h, Nile Red was completely released from particles produced by agitation and 85.64 ± 2.48% of the lipophilic dye was released from nanoparticles produced with sonication. In turn, after 24h, only 50.80 ± 1.37 %, for particles produced by agitation, and 40.87 ± 2.36 %, for particles produced sonication, of the hydrophilic dye was released from PLA nanoparticles. According to Rancan *et al.* (2009), upon contact with IPM, due to its low

dielectric constant that drastically reduces the electrostatic forces responsible for the stabilization of the colloid in the water phase, the PLA-NPs aggregates and irreversible forms clusters at the interface between water and IPM. Then, the organic phase penetrates within the PLA matrix [45]. For lipophilic compounds, such as Nile Red, since it has affinity to the lipophilic solvent, the partion of the dye between the lipophilic core of the particles and the lipophilic solvent occurred, leading to a rapidly diffusion to the outside of particles [45]. The rapid dye leakage also contributed to the destabilization of the particles that leads to the loss of the particulate state, which promoted a further increase in the release of the loaded dye [100]. For particles loaded with FITC, since this compound has poor solubility in the lipophilic solvent, a slow dissolution rate was achieved leading to a slowly diffusion out of the particles. This slow diffusion also had a stabilizing effect, and as a consequence of their higher stability, there was no destabilization of particles, preventing a fast release and resulting in prolonged fluorochrome release kinetics [70, 100].

Attending to the results obtained, and the results of other authors published on the literature, for Nile Red it was hypothesized that release occurs as function of diffusion and polymeric matrix degradation whereas for FITC, diffusion seems to control the release of hydrophilic compounds. To confirm these predictions, the empirical expression proposed by Ritger-Peppas was used to determine the mechanism of drug release from polymeric nanoparticles produced in this work; this equation is based on the Fickian diffusion equation [101]. For a sphere, a Fickian diffusion of first order is observed when *n* has the limiting value of 0.43. Between 0.43 and 0.85, anomalous transport is observed coupling Fickian diffusion and polymer degradation. Finally, for *n*=0.85, Case II transport (polymer relaxation/degradation) occurs, leading to a zero-order release [84].

For PLA nanoparticles produced in this work, the *n* value obtained for the tested dyes are shown in Table 4-4. For all the *n* values obtained, the correlation coefficient "R^2" was above the permissible range (0.95), further supporting the validity of the results. As expected, for Nile Red, the drug transport mechanism obtained was Non-Fickian diffusion or Anomalous, indicating the superposition of both extreme phenomena: drug diffusion and macromolecular chain relaxation/degradation. For

FITC, a Fickian diffusion of first order was achieved. Once again, these results indicate that the type of compound entrapped in the nanoparticles influences the drug transport mechanism.

Table 4-4: Dye release kinetic data obtained from fitting experimental release data to Ritger-Peppas Equation, where "*n*" is the diffusion exponent and R^2 is the correlation coefficient.

	Nile Red		FITC	
	n	**R^2**	***n***	**R^2**
Agitation	0.847	0.993	0.209	0.959
Sonication	0.728	0.988	0.124	0.987

4.5. Follicular Penetration of PLA Nanoparticles

In order to confirm that nanoparticles obtained in this work can act as carriers for drug delivery into the hair follicles, after application of PLA-NPs loaded with lipophilic (Nile Red) and hydrophilic (FITC) fluorochromes on porcine skin, the samples were sectioned and analyzed with fluorescence microscopy. The results obtained are reported in Figure 4-9.

Attending to the images, it is possible to note the presence of the fluorochromes inside the HFs, with fluorescence being detected along the entire length of the follicular duct. On the other hand, no fluorescence is observed in the viable epidermis. These results are in accordance with the findings of other authors, which showed that the encapsulation of compounds inside nanoparticles prevents their penetration on the skin through the transepidermal pathway, since NPs tends to penetrate along the follicular ducts, being trapped inside these structures [45, 75,

100]. Despite PLA-NPs did not reach the dermis, the results obtained shows that a great amount of them accumulated in the *stratum corneum*, failing to penetrate into the hair follicles. This behavior of NPs can be explained by the fact that no massage was applied on the skin samples after contact with the formulation. In the literature is reported that massage can simulate the hair movement that occurs physiologically under *in vivo* conditions and, once the moving hairs acts as a geared pump pushing particles deeply into the hair follicles, it enhances the penetration of NPs [37, 49].

Comparing the results obtained for NPs produced with agitation and sonication, it is possible to note that the distribution of Nile Red along the follicular duct was the same with the dye being detected at the deepest portion of the follicular duct. This similar penetration profile was already expected since particles obtained with both methodologies had comparable properties. However, the fluorescence was less intense around the hair follicles of skin samples where PLA-NPs produced with sonication were applied. As the concentration of particles in the formulation obtained with ultrasound is lower than those obtained with agitation (as demonstrated previously, formulation produced with ultrasound has lower yield), less particles were available to penetrate the HFs, which can explain the difference in the results obtained.

Finally, and contrary to the expected, FITC loaded PLA-NPs did not show a deeper penetration when compared to particles loaded with Nile Red. As seen before, since FITC has less affinity for lipophilic mediums (e.g., skin or sebum inside the hair follicles), it diffuses slowly out of the particles, promoting a stabilizing effect that enhances the penetration of these particles [100]. In turn, after the entrance of Nile Red loaded NPs into the follicular ducts, a destabilization of the particles due to the contact with the sebum and a fast release of the entrapped compound occur. Consequently, the destabilized particles tend to accumulate in the upper part of the follicular duct. Since this study did not allow to determine unequivocally that fluorescence in the follicles was due to the particles with the dyes entrapped, it is possible that released Nile Red had diffuse alone via the sebum to the deepest part of the HFs and the fluorescence detected was due to the dye itself and not because of the accumulation of particles at this level [45, 100].

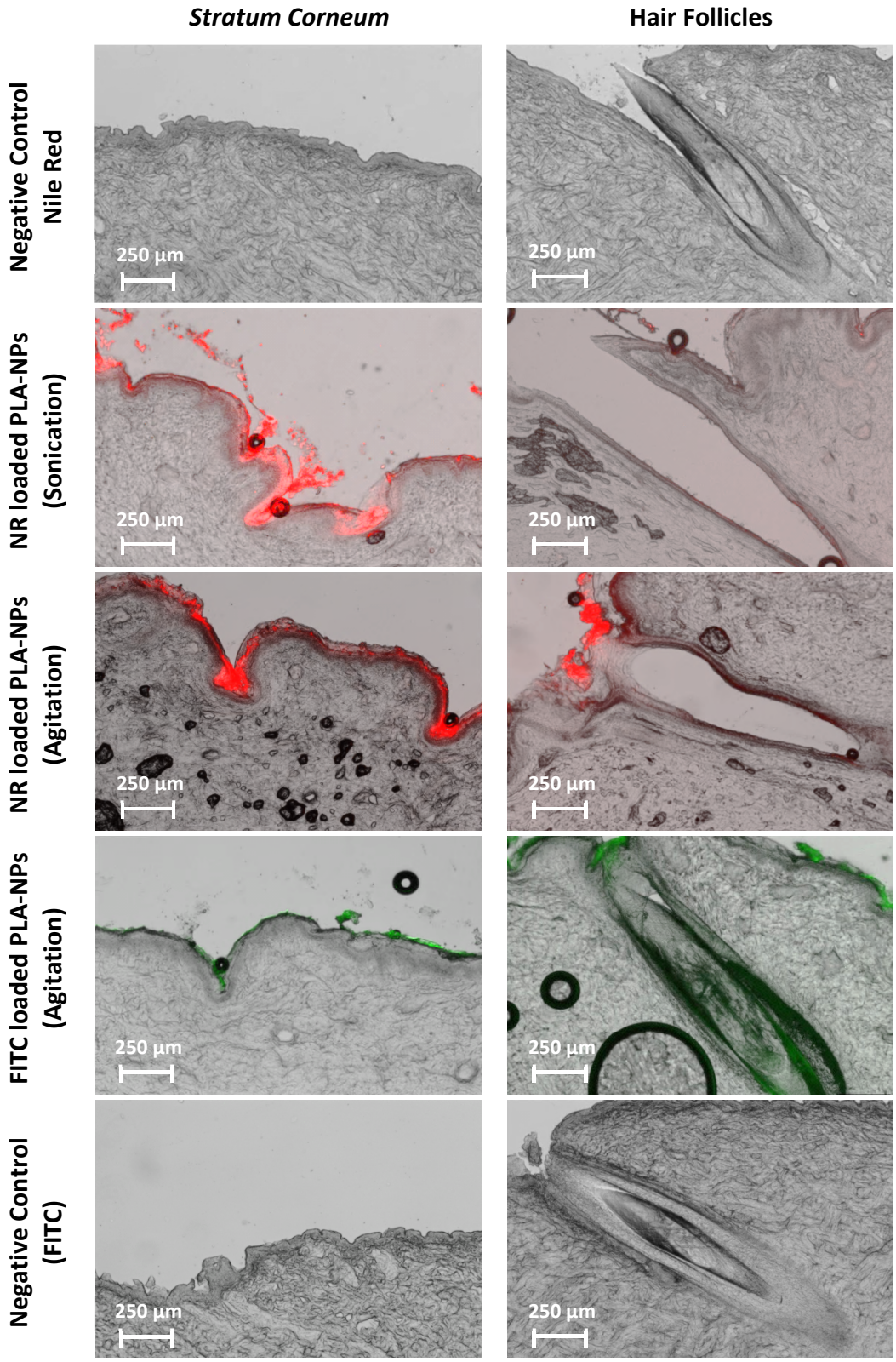

Figure 4-9: **Fluorescence microscopy images (x5 magnification) of porcine skin cryosections, after incubation with dye loaded PLA-NPs.**

5. CONCLUSIONS AND FUTURE PERSPECTIVES

In this study, the use of agitation, sonication or homogenization along with the standard nanoprecipitation method allowed the successful preparation of PLA particles in the range of nanometers. Using acetone as the solvent phase, agitation proved to be the most suited technique to obtain carriers for follicular targeting since it produced the smallest particles with the narrowest size distribution without the use of higher energy apparatus (making it easier to scale-up). Nevertheless, since the mean size of particles obtained with agitation and sonication was not so different, the employment of ultrasound was also considered because it allows the preparation of PLA-NPs much faster than agitation (18 min instead of one night). Furthermore, it is well reported in literature the ability of sonication, compared with other techniques, to achieve high drug loadings in the emulsification-solvent evaporation method [39]. If in the progress of this work, the same ability could be proved for nanoprecipitation, the use of ultrasound could become very competitive with mechanical stirring for the production of drug loaded PLA-NPs.

As expected, the choice of a good solvent phase is crucial for the quality of PLA nanoparticles produced by nanoprecipitation. Particularly, a fraction of a suitable non-solvent (chosen on the basis of its polarity and upon the affinity of polymer to it) in the solvent phase can favor the elaboration of particles with smaller sizes as seen for the mixture Acetone/Ethanol. It is important to note that, despite the variations obtained with other organic phases, no significant differences were found on the mean size of particles produced with agitation and sonication when the mixture Acetone/Ethanol was employed. Conversely, increasing the amount of Pluronic F68 does not decrease the size of PLA nanoparticles and the minimal tested concentration - 0.6% (w/w) - produced the smallest particles. In turn, particles with higher homogeneity were obtained until a maximum of 1.5% (w/w) of surfactant. However, the choice of the best concentration for the production of nanoparticles was made attending to the concentration that provided the smaller sizes and not the lower polydispersity. This occurred because, for 0.6% (w/w) of Pluronic F68, the homogeneity of solutions was already adequate and it is known that as the concentration of stabilizer increases, the drug incorporation can be drastically reduced due to the interaction between drug and stabilizer [69, 92].

In terms of the nanoparticles formation, higher yields can be obtained using agitation instead of sonication. Also, as the volume fraction of ethanol in the solvent phase increases, the yield of nanoparticles decreases. Nevertheless, the lowest ethanol fraction (45%) promoted negative changes on the properties of nanoparticles; for sonication led to an increase on the mean diameter of particles, whereas for agitation the stability was compromised. Once the size, PDI and ζ-potential of particles produced with the other two tested fraction of ethanol (50% and 55%) do not had noteworthy differences and 50% promoted a yield of nanoparticles closer to that obtained with 45%, Acetone/Ethanol (50/50, v/v) was assumed as the optimal mixture for the production of PLA nanoparticles.

Taking into account the desired properties of particles for follicular targeting, as well as the yield necessary for the commercial viability of a formulation, as intended, at the end of the first part of this work, suitable formulations for the production of PLA-NPs by nanoprecipitation were obtained. In the future, an upgrading in the production must be conducted in order to understand if properties of nanoparticles are not severely affected by the transition from laboratory to large-scale production. Despite being produced from a material that is biocompatible, since the produced PLA nanoparticles are intended for cosmetic applications in humans, an evaluation of its cytotoxicity is also one of the next steps of this project.

The two methodologies for nanoprecipitation (using agitation and sonication), presented in this work, demonstrates the ability to efficiently entrap lipophilic compounds (Nile Red), but most important, the results obtained reflect the underexplored potential of the method to entrap compounds of hydrophilic nature (FITC). Also, although the entrapment efficiency for both dyes was slightly lower for sonication, the use of ultrasound systems promoted higher loading efficiencies (amount of entrapped compound compared to the effective mass of nanoparticles), confirming the expectations for this technique. For drug delivery, this is an advantage since a successful NP system may be the one which has a high loading capacity, reducing the quantity of the carrier required for administration [62]. Regarding to the release from PLA-NPs, it was shown to be dependent upon the nature of the encapsulated compound, as well as upon its loading into nanoparticles. Using lipophilic

molecules, the release is faster when compared to the hydrophilic ones. For a given compound, a faster release is achieved using NPs produced with agitation (lower dye loading) and if it is necessary a slower release, the compounds can be incorporated in particles produced with sonication (higher dye loading). As a future task, the production of PLA-NPs loaded with other lipophilic and hydrophilic compounds (namely, drugs for the treatment of hair follicle diseases/disorders) will be performed to determine their entrapment efficiency as well as their *in vitro* release profile and drug release kinetics, in order to validate the results obtained with the lipophilic (Nile Red) and hydrophilic (FITC) model compounds used in this study.

After *in vitro* studies of follicular penetration, it was confirmed that PLA-NPs produced with agitation or sonication are equally capable to enhance the transport molecules into the HFs. Moreover, these nanocarriers also proved to be well suited for the delivery of lipophilic and hydrophilic model compounds into HFs, with the fluorochromes achieving a maximal depth classified as deep penetration (level of functional structures as the hair bulb). While the doubts whether the detected fluorescence inside the HFs is due to particles or from the free dye (after release from PLA-NPs) remains, what it is important to note is that, using the particles produced in this work, the dyes were effectively incorporated into the HFs. After these preliminary results, other experiments of follicular penetration will be performed with formulations containing the same concentration of PLA-NPs (avoiding some defaults of the experimental design used) and applying massage to the skin samples in order to better simulate the *in vivo* conditions imposed by the HFs for the penetration of topically applied nanoparticles.

Gathering all the results obtained, PLA-NPs produced in this work represent ideal candidates for the encapsulation of different drugs that needed to be delivery into the HFs. Then, these NPs may be used in cosmetic applications to enhance the treatment of many hair follicles associated disorders/diseases.

6. REFERENCES

[1] Shoseyov O. and Levy I. (2008). *Nanomedicine, Nanopharmaceutical and Nanosensing in Nanobiotechnology - Bioinspired Devices and Materials of the Future.* Humana Press: Totowa, New Jersey p. 485.

[2] Jun J.Y., *et al.* (2011). *Preparation of size-controlled bovine serum albumin (BSA) nanoparticles by a modified desolvation method.* Food Chemistry 127(4): 1892-1898.

[3] Cevc G. and Vierl U. (2010). *Nanotechnology and the transdermal route: A state of the art review and critical appraisal.* Journal of Controlled Release 141(3): 277-299.

[4] Mihranyan A., Ferraz N. and Strømme M. (2012). *Current status and future prospects of nanotechnology in cosmetics.* Progress in Materials Science 57(5): 875-910.

[5] Morganti P. (2010). *Use and potential of nanotechnology in cosmetic dermatology.* Clinical, Cosmetic and Investigational Dermatology 3: 5-13.

[6] Kabri T., *et al.* (2011). *Physico-chemical characterization of nanoemulsions in cosmetic matrix enriched on omega-3.* Journal of Nanobiotechnology 9: 41.

[7] Padamwar M.N. and Pokharkar V.B. (2006). *Development of Vitamin Loaded Liposomal Formulations Using Factorial Design Approach: Drug Deposition and Stability.* International Journal of Pharmaceutics 320(1-2): 37-44.

[8] Prausnitz M.R. and Langer R. (2008). *Transdermal drug delivery.* Nature Biotechnology 26(11): 1261-1268.

[9] Schäfer-Korting M, Mehnert W. and Korting H.C. (2007). *Lipid nanoparticles for improved topical application of drugs for skin diseases.* Advanced Drug Delivery Reviews 59(6): 427-443.

[10] Araújo R., *et al.* (2010). *Biology of Human Hair: Know Your Hair to Control It*. Advances in Biochemical Engineering/Biotechnology 125: 121-143.

[11] Papakostas D., *et al.* (2011). *Nanoparticles in dermatology*. Archives of Dermatological Research 303(8): 533-550.

[12] Shi J., *et al*. (2010). *Nanotechnology in Drug Delivery and Tissue Engineering: From Discovery to Applications.* Nano Letters 10(9): 3223-3230.

[13] Hughes G.A. (2005). *Nanostructure-mediated drug delivery*. Nanomedicine: Nanotechnology, Biology, and Medicine 1(1): 22-30.

[14] Prow T.W., *et al.* (2011). *Nanoparticles and microparticles for skin drug delivery.* Advanced Drug Delivery Reviews 63(6): 470-491.

[15] Gomes V.M.A. (2009). *Encapsulação de Ciprofloxacina em nanopartículas de poli(ácido láctico).* Master Thesis in Analytical Chemistry and Quality Control, University of Aveiro.

[16] Freiberg S. and Zhu X.X. (2004). *Polymer microspheres for controlled drug release.* International Journal of Pharmaceutics 282(1-2): 1-18.

[17] Mu L. and Sprando R.L. (2010). *Application of Nanotechnology in Cosmetics.* Pharmaceutical Research 27(8): 1746-1749.

[18] Hirsjärvi S. (2008). *Preparation and Characterization of Poly(Lactic Acid) Nanoparticles for Pharmaceutical Use.* Doctoral Dissertation, University of Helsinki.

[19] Das S., *et al.* (2011). *Nanotechnology in oncology: Characterization and in vitro release kinetics of cisplatin-loaded albumin nanoparticles: Implications in anticancer drug delivery.* Indian Journal of Pharmacology 43(4): 409-413.

[20] Silva R. (2011). *Sonoproduction of particles for delivery purposes.* Doctoral Thesis in Textile Engineering, University of Minho.

[21] Schneider M., *et al.* (2009). *Nanoparticles and their interactions with the dermal barrier.* Dermato-endocrinology 1(4): 197-206.

[22] Guterres S.S., Alves M.P. and Pohlmann A.R. (2007). *Polymeric Nanoparticles, Nanospheres and Nanocapsules for Cutaneous Applications.* Drug Target Insights 2: 147-157.

[23] Tsallas A.T. (2010). *Bladder Tissue Distribution of Paclitaxel and Docetaxel from polymeric nanoparticles.* Master Thesis in Pharmaceutical Sciences, University of Toronto.

[24] Ataman-Önal Y., *et al.* (2006). *Surfactant-free anionic PLA nanoparticles coated with HIV-1 p24 protein induced enhanced cellular and humoral immune responses in various animal models.* Journal of Controlled Release 112(2): 175-185.

[25] Garala K.C., Shinde A.J. and Shah P.H. (2009). *Formulation and in vitro characterization of monolithic matrix transdermal systems using HPMC/EUDRAGIT S 100 polymer blends.* International Journal of Pharmacy and Pharmaceutical Sciences 1(1): 108-120.

[26] Wu X. (2008). *Characterization and evaluation of novel nano/meso-particulate formulations for application to the skin.* Doctoral Thesis in Philosophy, University of Bath.

[27] Huzil J.T., *et al.* (2011). *Drug delivery through the skin: molecular simulations of barrier lipids to design more effective noninvasive dermal and transdermal delivery systems for small molecules, biologics, and cosmetics.* Wiley Interdisciplinary Reviews: Nanomedicine and Nanobiotechnology 3(5): 449-462.

[28] Jain J., Bhandari A. and Shah D. (2010). *Novel Carriers for Transdermal Drug Delivery: A Review.* International Journal of Pharmaceutical and Applied Sciences 1(2): 62-69.

[29] Anitha P., *et al.* (2011). *Ethosomes - A noninvasive vesicular carrier for transdermal drug delivery.* International Journal of Review in Life Sciences 1(1): 17-24.

[30] Thomas B.J. and Finnin B.C. (2004). *The transdermal revolution.* Drug Discovery Today 9(16): 697-703.

[31] Benson H.A. (2005). *Transdermal Drug Delivery: Penetration Enhancement Techniques.* Current Drug Delivery 2(1): 23-33.

[32] Sonavanea G., *et al.* (2008). *In vitro permeation of gold nanoparticles through rat skin and rat intestine: Effect of particle size.* Colloids and Surfaces B, Biointerfaces 65(1): 1-10.

[33] Alvarez-Román R., *et al.* (2004). *Enhancement of Topical Delivery from Biodegradable Nanoparticles.* Pharmaceutical Research 21(10): 1818-1825.

[34] Gillet A., *et al.* (2011). *Liposome surface charge influence on skin penetration behavior.* International Journal of Pharmaceutics 411(1-2): 223-231.

[35] Walters K.A. and Roberts M.S. (2002). *The structure and function of skin in Dermatological and Transdermal Formulations: Drugs and the Pharmaceutical Sciences*. Marcel Dekker Inc., New York, p. 1-39.

[36] Desai P., Patlolla R.R. and Singh M. (2010). *Interaction of nanoparticles and cell-penetrating peptides with skin for transdermal drug delivery.* Molecular Membrane Biology 27(7): 247-259.

[37] Contreras J. (2007). *Human Skin Drug Delivery using Biodegradable PLGA-nanoparticles.* Doctoral Thesis in Chemical, Pharmaceutical, Biotechnology and Materials Science, University of Saarland.

[38] Touitou E. (1998). *Composition of applying active substance to or through the skin.* US patent 5540934.

[39] Moghimi H.R., Williams A.C. and Barry B.W. (1996). *A lamellar matrix model for stratum corneum intercellular lIpids: Effect of geometry of the stratum corneum on permeation of model drugs 5-fluorouracil and oestradiol.* International Journal of Pharmaceutics 131(2): 117-129.

[40] Landmann L. (1986). *Epidermal permeability barrier: transformation of lamellar granule-disks into intercellular sheets by a membrane-fusion process, a freeze-fracture study.* Journal of Investigative Dermatology 87(2): 202-209.

[41] Gaur P.K., *et al.* (2009). *Transdermal Drug Delivery System: A Review.* Asian Journal of Pharmaceutical and Clinical Research 2(1): 14-20.

[42] Prausnitz M.R., Mitragotri S. and Langer R. (2004). *Current status and future potential of transdermal drug delivery.* Nature Reviews, Drug Discovery 3(2): 115-124.

[43] Feldmann R.J. and Maibach H.I. (1967). *Regional variation in percutaneous penetration of 14C cortisol in man.* Journal of Investigative Dermatology 48(2): 181-183.

[44] Jung S., *et al.* (2006). *Innovative Liposomes as a Transfollicular Drug Delivery System: Penetration into Porcine Hair Follicles.* Journal of Investigative Dermatology 126(8): 1728-1732.

[45] Rancan F., *et al.* (2009). *Investigation of Polylactic Acid (PLA) Nanoparticles as Drug Delivery Systems for Local Dermatotherapy.* Pharmaceutical Research 26(8): 2027-2036.

[46] Meidan V.M., Bonner M.C. and Michniak B.B. (2005). *Transfollicular drug delivery—Is it a reality?.* International Journal of Pharmaceutics 306(1-2): 1-14.

[47] Lauer A.C., *et al.* (1995). *Transfollicular drug delivery.* Pharmaceutical Research 12(2): 179-186.

[48] Lademann J., *et al.* (2007). *Nanoparticles – An efficient carrier for drug delivery into the hair follicles.* European Journal of Pharmaceutics and Biopharmaceutics 66(2): 159-164.

[49] Lademann J., *et al.* (2011). *Penetration and storage of particles in human skin: Perspectives and safety aspects.* European Journal of Pharmaceutics and Biopharmaceutics 77(3): 465-468.

[50] Mak W.C., *et al.* (2012). *Triggering of drug release of particles in hair follicles.* Journal of Controlled Release. 160(3): 509-514.

[51] Konrádsdóttir F., Sigurdsson V. and Loftsson T. (2009). *Drug Targeting to the Hair Follicles: A Cyclodextrin-Based Drug Delivery.* AAPS PharmaSciTech 10(1): 266-269.

[52] Wosicka H. and Cal K. (2010). *Targeting to the hair follicles: Current status and potential.* Journal of Dermatological Science 57(2): 83-89.

[53] Hoffman R.M. (2006). *The hair follicle and its stem cells as drug delivery targets.* Expert Opinion on Drug Delivery 3(3): 437-443.

[54] Patzelt A., *et al.* (2011). *Influence of the Vehicle on the Penetration of Particles into Hair Follicles.* Pharmaceutics 3(2): 307-314.

[55] Morgen M., *et al.* (2011). *Targeted delivery of a poorly water-soluble compound to hair follicles using polymeric nanoparticle suspensions.* International Journal of Pharmaceutics 416(1): 314-322.

[56] Golubovic-Liakopoulos N., Simon S.R. and Shah B. (2011). *Nanotechnology Use with Cosmeceuticals.* Seminars in Cutaneous Medicine and Surgery 30(3): 176-180.

[57] Murakami H., Kobayashi M. and Takeuchi H. (1999). *Preparation of poly(DL-lactide-co-glycolide) nanoparticles by modified spontaneous emulsification solvent diffusion method.* International Journal of Pharmaceutics 187(2): 143-152.

[58] Liu M., *et al.* (2005). *Characterization and release of triptolide-loaded poly (D,L-lactic acid) nanoparticles.* European Polymer Journal 41(2): 375-382.

[59] Singh V., *et al.* (2008). *Synthesis of Polylactide with Varying Molecular Weight and Aliphatic Content: Effect on Moisture Sorption.* Master Thesis in Chemical Engineering, University of Drexel.

[60] Garlotta D. (2001). *A Literature Review of Poly(Lactic Acid).* Journal of Polymers and the Environment 9(2): 63-84.

[61] Belbella A., *et al.* (1996). *In vitro degradation of nanospheres from poly(D,L-lactides) of different molecular weights and polydispersities.* International Journal of Pharmaceutics 129(1-2): 95-102.

[62] Soppimatha K.S., *et al.* (2001). *Biodegradable polymeric nanoparticles as drug delivery devices.* Journal of Controlled Release 70(1-2): 1-20.

[63] Niwa T., *et al.* (1993). *Preparation of biodegradable nanospheres of water soluble and insoluble drugs with D,L-lactide:glycolide copolymer by a novel spontaneous emulsification solvent diffusion method, and the drug release behavior.* Journal of Controlled Release 25(1-2): 89-98.

[64] Allemann E., Gurnay R. and Doelker E. (1992). *Preparation of aqueous polymeric nanodispersions by a reversible salting-out process: influence of process parameters on particle size.* International Journal of Pharmaceutics 87(1-3): 247-253.

[65] Makadia H.K. and Siegel S.J. (2011). *Poly Lactic-co-Glycolic Acid (PLGA) as Biodegradable Controlled Drug Delivery Carrier.* Polymers 3(3): 1377-1397.

[66] Fessi H., *et al.* (1986). *Process for the preparation of dispersible colloidal systems of a substance in the form nanoparticles.* US Patent 5118528.

[67] Lee Y.H., *et al.* (2010). *Release profile characteristics of biodegradable-polymer-coated drug particles fabricated by dual-capillary electrospray.* Journal of Controlled Release 145(1): 58-65.

[68] Legrand P., *et al.* (2007). *Influence of polymer behaviour in organic solution on the production of polylactide nanoparticles by nanoprecipitation.* International Journal of Pharmaceutics 344(1-2): 33-43.

[69] Hans M.L. and Lowman A.M. (2002). *Biodegradable nanoparticles for drug delivery and targeting.* Current Opinion in Solid State and Materials Science 6(4): 319-327.

[70] Leo E., *et al.* (2004). *In vitro evaluation of PLA nanoparticles containing a lipophilic drug in water-soluble or insoluble form.* International Journal of Pharmaceutics 278(1): 133-141.

[71] Tsujimoto H., *et al.* (2007). *Evaluation of the permeability of hair growing ingredient encapsulated PLGA nanospheres to hair follicles and their hair growing effects.* Bioorganic & Medicinal Chemistry Letters 17(17): 4771-4777.

[72] Shim J., *et al.* (2004). *Transdermal delivery of mixnoxidil with block copolymer nanoparticles.* Journal of Controlled Release 97(3): 477-484.

[73] Mansberger S.L. and Cioffi G.A. (2000). *Eyelash formation secondary to latanoprost treatment in a patient with alopecia.* Archives of Ophthalmology 118(5): 718-719.

[74] Johnstone M.A. (1997). *Hypertrichosis and increased pigmentation of eyelashes and adjacent hair in the region of the ipsilateral eyelids of patients treated with unilateral topical latanoprost.* American Journal of Ophthalmology 124(4): 544-547.

[75] Vogt A., *et al.* (2006). *40 nm, but not 750 or 1500 nm, nanoparticles enter epidermal CD1a+ cells after transcutaneous application on human skin.* Journal of Investigative Dermatology 126(6): 1316-1322.

[76] Hampson J.P., *et al.* (1995). *Tamoxifen-induced hair colour change.* British Journal of Dermatology 132(3): 483-484.

[77] Mansour H.M., *et al.* (2010). *Materials for Pharmaceutical Dosage Forms: Molecular Pharmaceutics and Controlled Release Drug Delivery Aspects.* International Journal of Molecular Sciences 11(9): 3298-3322.

[78] Xin-yu J., Chun-shan Z. and Ke-wen T. (2003). *Preparation of PLA and PLGA nanoparticles by binary organic solvent diffusion method.* Journal of Central South University Technology 10(3): 202-206.

[79] Greenspan P. and Fowler D. (1985). *Spectrofluorometric studies of the lipid probe, nile red.* Journal of Lipid Research 26(7): 781-789.

[80] Gaucher G., *et al.* (2007). *Poly(N-Vinyl-Pyrrolidone)-Block-Poly(D,L-Lactide) as Polymeric Emulsifier for the Preparation of Biodegradable Nanoparticles.* Journal of Pharmaceutical Sciences 96(7): 1763-1775.

[81] Hammond S.A., *et al.* (2000). *Transcutaneous immunization of domestic animals: opportunities and challenges.* Advanced Drug Delivery Reviews 43(1): 45-55.

[82] Silva R., *et al.* (2010). *Effect of ultrasound parameters for unilamellar liposome preparation.* Ultrasonics Sonochemistry 17(3): 628–632.

[83] Santander-Ortega M.J., *et al.* (2006). *Colloidal stability of Pluronic F68-coated PLGA nanoparticles: A variety of stabilisation mechanisms.* Journal of Colloid and Interface Science 302(2): 522–529.

[84] Silva R., *et al.* (2012). *Protein microspheres as suitable devices for piroxicam release.* Colloids and Surfaces B, Biointerfaces 92: 277-285.

[85] Silva C., *et al.* (2012). *Characterization of sono and hydrodynamic reactors for laccase cotton bleaching.* (Submitted to Ultrasonics Sonochemistry).

[86] Schubert S., Delaney J.T. and Schubert U.S. (2011). *Nanoprecipitation and nanoformulation of polymers: from history to powerful possibilities beyond poly(lactic acid)*. Soft Matter 7(5): 1581–1588.

[87] Bilati U., Doelker E. and Allémann E. (2005). *Development of a nanoprecipitation method intended for the entrapment of hydrophilic drugs into nanoparticles.* European Journal of Pharmaceutical Sciences 24(1): 67–75.

[88] Wischke C. and Schwendeman S.P. (2008). *Principles of encapsulating hydrophobic drugs in PLA/PLGA microparticles.* International Journal of Pharmaceutics 364(2): 298-327.

[89] Peltonen L., *et al.* (2002). *The Effect of Cosolvents on the Formulation of Nanoparticles From Low-Molecular-Weight Poly(l)lactide.* AAPS PharmSciTech 3(4): E32.

[90] Guhagarkar S.A., Malshe V.C. and Devarajan P.V.(2009). *Nanoparticles of Polyethylene Sebacate: A New Biodegradable Polymer.* AAPS PharmSciTech, 10(3): 935-942.

[91] McGinity J.W. and O'Donnell P.B. (1997). *Preparation of microspheres by the solvent evaporation technique.* Advanced Drug Delivery Reviews 28(1): 25-42.

[92] Mao S., *et al.* (2007). *Effect of WOW process parameters on morphology and burst release of FITC-dextran loaded PLGA microspheres.* International Journal of Pharmaceutics 334(1-2): 137-148.

[93] Vandervoort J. and Ludwig A. (2001). *Preparation factors affecting the properties of polylactide nanoparticles: A factorial design study.* Die Pharmazie 56(6): 484-488.

[94] Zweers M.L., *et al.* (2003). *The Preparation of Monodisperse Biodegradable Polyester Nanoparticles with a Controlled Size.* Journal of Biomedical Materials Research Part B, Applied Biomaterials 66(2): 559-566.

[95] Xu Y. and Du Y. (2003). *Effect of Molecular Structure of Chitosan on Protein Delivery Properties of Chitosan Nanoparticles.* International. Journal of Pharmaceutics 250(1): 215-226.

[96] Cao T., Gao X. and Gu Y. (2007). *Biodegradable polylactide microspheres containing anticancer drugs used as injectable drug delivery system.* IEEE/ICME International Conference on Complex Medical Enginnering.

[97] Jeong Y., *et al.* (2002). *Testosterone-encapsulated Surfactant-free Nanoparticles of Poly(DL-lactide-co-glycolide): Preparation and Release Behavior.* Bulletin of the Korean Chemistry Society 23(11): 1579-1584.

[98] Polakovic M., *et al.* (1999). *Lidocaine loaded biodegradable nanospheres. II. modeling of drug release.* Journal of Controlled Release 60(2-3): 169-177.

[99] Chawla J.S. and Amiji M.M. (2002). *Biodegradable poly(o-caprolactone) nanoparticles for tumortargeted delivery of tamoxifen.* International Journal of Pharmaceutics 249(1-2): 127-138.

[100] Rancan F., *et al.* (2012). *Stability of polylactic acid particles and release of fluorochromes upon topical application on human skin explants.* European Journal of Pharmaceutics and Biopharmaceutics 80(1): 76-84.

[101] Ritger P.L and Peppas N.A. (1987). *A Simple Equation for Description of Solute Release I. Fickian and Non-Fickian Release from Non-Swellable Devices in the form of Slabs, Spheres, Cylinders or Discs.* Journal of Controlled Release 5(1): 23-36.